FINAL REPORT
SOLID LUBRICATED SILICON NITRIDE BEARINGS AT HIGH SPEED AND TEMPERATURE - PHASE 1
N00019-80-C-0565

T. M. YONUSHONIS

FEBRUARY 2, 1982

Approved for public release: distribution unlimited

Prepared for:

U. S. DEPARTMENT OF THE NAVY
NAVAL AIR SYSTEMS COMMAND (AIR-5304C1)
WASHINGTON, D.C. 20361

SKF TECHNOLOGY SERVICES
SKF INDUSTRIES, INC

SECURITY CLASSIFICATION OF THIS PAGE (When Data Entered)

REPORT DOCUMENTATION PAGE

READ INSTRUCTIONS BEFORE COMPLETING FORM

1. REPORT NUMBER: AT82D002	2. GOVT ACCESSION NO.: AD-A114848
3. RECIPIENT'S CATALOG NUMBER:	
4. TITLE (and Subtitle): SOLID LUBRICATED SILICON NITRIDE BEARINGS AT HIGH SPEED AND TEMPERATURE - PHASE I	5. TYPE OF REPORT & PERIOD COVERED: FINAL REPORT Sept. 1980 - October 1981
	6. PERFORMING ORG. REPORT NUMBER: AT82D002
7. AUTHOR(s): T. M. YONUSHONIS	8. CONTRACT OR GRANT NUMBER(s): N00019-80-C-0565
9. PERFORMING ORGANIZATION NAME AND ADDRESS: SKF INDUSTRIES, INC. 1100 FIRST AVENUE KING OF PRUSSIA, PA. 19406	10. PROGRAM ELEMENT, PROJECT, TASK AREA & WORK UNIT NUMBERS:
11. CONTROLLING OFFICE NAME AND ADDRESS: DEPARTMENT OF THE NAVY NAVAL AIR SYSTEMS COMMAND (AIR-5304C1) WASHINGTON D.C. 20361	12. REPORT DATE: FEBRUARY 1982
	13. NUMBER OF PAGES: 67
14. MONITORING AGENCY NAME & ADDRESS (if different from Controlling Office): DEFENSE CONTRACT ADMINISTRATION SERVICES MANAGEMENT AREA PHILADELPHIA P.O. BOX 7699 PHILADELPHIA, PA 19101	15. SECURITY CLASS. (of this report): UNCLASSIFIED
	15a. DECLASSIFICATION/DOWNGRADING SCHEDULE:

16. DISTRIBUTION STATEMENT (of this Report)

APPROVED FOR PUBLIC RELEASE, DISTRIBUTION UNLIMITED

17. DISTRIBUTION STATEMENT (of the abstract entered in Block 20, if different from Report)

18. SUPPLEMENTARY NOTES

19. KEY WORDS (Continue on reverse side if necessary and identify by block number)

BEARINGS
CAGE DESIGN
GRAPHITE
HIGH SPEED
HIGH TEMPERATURE
HOT PRESSED SILICON NITRIDE
SOLID LUBRICATION

20. ABSTRACT (Continue on reverse side if necessary and identify by block number)

Functional evaluations of solid lubricated 7205 bearings were conducted over the speed range, 10,000 rpm (1050 rad/sec) to 55,000 rpm (5760 rad/sec), using an air turbine drive system. The 7205 bearings were comprised of silicon nitride balls, M50 steel rings, and graphite containing cages. Graphite films transferred from the cage to the ball surfaces, then to the groove surfaces were the only source of lubrication. Liquid lubrication was not

DD FORM 1 JAN 73 1473 EDITION OF 1 NOV 65 IS OBSOLETE

SECURITY CLASSIFICATION OF THIS PAGE (When Data Entered)

supplied to the test bearings.

Successful steady-state operation of the 7205 bearings containing a three piece outer land riding graphite cage was limited to less than 25,000 rpm (2880 rad/sec) at the axial loads selected, 25 lbf (110 N) and 100 lbf (445 N). Heat generated from the solid lubricated rolling and sliding contacts was not removed from the inner ring as rapidly as the heat removed from the outer ring which resulted in a temperature differential between the inner and outer rings. Test bearing seizure occurred rapidly due to this thermal gradient as the turbine drive was accelerated beyond 25,000 rpm. Attempts to improve bearing performance at the higher speeds by increasing the cooling air flow, increasing the bearing housing temperature, decreasing load, and increasing the bearing diametral clearance were unsuccessful.

The three piece graphite cage, drawing number L-23845, could survive acceleration of the bearing inner ring to 55,000 rpm (5760 rad/sec) without damage. These tests were accomplished by rapidly accelerating the air turbine to 55,000 rpm in less than 15 seconds, then rapidly decreasing the turbine air supply.

An inner ring riding stainless steel shrouded graphite cage, drawing number L-23846, was found to be unstable due to the lack of dampening and insufficient axial piloting.

Thermal analysis of the bearing system did not predict bearing seizure at the test conditions selected. Further studies of the bearing system revealed that if a slightly higher heat generation rate was assumed, then bearing seizure would occur due to unstable bearing temperatures. The increase in heat generated required to result in bearing seizure, approximately 10 watts, could be accounted for by ball-cage pocket sliding.

Inspection of the bearing components after the tests was very encouraging. The graphite films transferred to the silicon nitride balls and M50 steel grooves were effective in preventing wear of the bearing surfaces. The cage pocket wear and wear of the graphite piloting surfaces were considered acceptable. Optical microscopy of etched M50 ring cross sections revealed that limited plastic deformation has occurred during the tests. Plastic deformation of the inner ring groove surface was believed to be significant, since plastic deformation would result in a higher heat generation at the inner ring surface contributing to bearing seizure. The silicon nitride balls did not exhibit any evidence of plastic deformation.

Table of Contents

Table of Contents - Continued

F-4185C-1-R100

Illustrations

Illustrations - Continued

Tables

Abstract:

Functional evaluations of solid lubricated 7205 bearings were conducted over the speed range, 10,000 rpm (1050 rad/sec) to 55,000 rpm (5760 rad/sec), using an air turbine drive system. The 7205 bearings were comprised of silicon nitride balls, M50 steel rings, and graphite containing cages. Graphite films transferred from the cage to the ball surfaces, then to the groove surfaces were the only source of lubrication. Liquid lubrication was not supplied to the test bearings.

Successful steady-state operation of the 7205 bearings containing a three piece outer land riding graphite cage was limited to less than 25,000 rpm (2880 rad/sec) at the axial loads selected, 25 lbf (110 N) and 100 lbf (445 N). Heat generated from the solid lubricated rolling and sliding contacts was not removed from the inner ring as rapidly as the heat removed from the outer ring which resulted in a temperature differential between the inner and outer rings. Test bearing seizure occurred rapidly due to this thermal gradient as the turbine drive was accelerated beyond 25,000 rpm. Attempts to improve bearing performance at the higher speeds by increasing the cooling air flow, increasing the bearing housing temperature, decreasing load, and increasing the bearing diametral clearance were unsuccessful.

The three piece graphite cage, drawing number L-23845, could survive acceleration of the bearing inner ring to 55,000 rpm (5760 rad/sec) without damage. These tests were accomplished by rapidly accelerating the air turbine to 55,000 rpm in less than 15 seconds, then rapidly decreasing the turbine air supply.

An inner ring riding stainless steel shrouded graphite cage, drawing number L-23846, was found to be unstable due to the lack of dampening and insufficient axial piloting.

Thermal analysis of the bearing system did not predict bearing seizure at the test conditions selected. Further studies of the bearing system revealed that if a slightly higher heat generation rate was assumed, then bearing seizure would occur due to unstable bearing temperatures. The increase in heat generated required to result in bearing seizure, approximately 10 watts, could be accounted for by ball-cage pocket sliding.

Inspection of the bearing components after the tests was very encouraging. The graphite films transferred to the silicon nitride balls and M50 steel grooves were effective in preventing wear of the bearing surfaces. The cage pocket wear and wear of the graphite piloting surfaces were considered acceptable. Optical microscopy of etched M50 ring cross sections revealed that

limited plastic deformation had occurred during the tests. Plastic deformation of the inner ring groove surface was believed to be significant, since plastic deformation would result in a higher heat generation at the inner ring surface contributing to bearing seizure. The silicon nitride balls did not exhibit any evidence of plastic deformation.

Preface:

This report presents the results of an experimental study which investigated solid lubrication of 7205 angular contact bearings at high speed. The solid lubricant was supplied to the bearing surfaces from the solid lubricant reservoir (graphite containing cage) by ball-cage pocket sliding. The work was conducted by SKF Technology Services, at SKF Industries, Inc., King of Prussia, Pennsylvania, for the U.S. Naval Air Systems Command, Washington D.C., 20361, under contract number N00019-80-C-0565. This report is the final technical report issued on the program entitled, "Solid Lubricated Silicon Nitride Bearings at High Speed and Temperature, Phase I." The program was conducted during the period extending from September 1980 to October 1981.

The author wishes to acknowledge the valuable contributions of SKF personnel consulted during the course of the program. The contributions of B. Carlson, R. Doyle, M. Ragen, M. Overholtzer, F. Morrison, and L. Sibley are greatly appreciated. The contributions of W. Rosenlieb in conducting and defining the experiments are gratefully acknowledged. The patient typing of this report by K. Helicher and A. Hindo is appreciated.

1.0 Introduction

1.1 Overview

Advancements in the performance of high speed turbomachinery require the rotating turbine components to operate at higher speeds and higher temperatures. The temperatures projected for the bearing locations of compact, limited life, high performance turbine engines exceed the capability of conventional lubrication systems and conventional metal bearing alloys. These high temperature bearing locations will require the development and use of a solid lubricated bearing.

SKF Industries with funding from the Naval Air Systems Command has been investigating [1, 2, 3] a bearing quality ceramic, hot pressed silicon nitride (HPSN), which has the potential to operate at the arduous service conditions projected by the engine manufacturers. Previous programs [2, 3] have demonstrated that the HPSN has an acceptable oil lubricated bearing fatigue life and that the material can be effectively lubricated by graphite transfer films at 1000°F (540°C).

Although these programs have demonstrated the silicon nitride fatigue life capability and effective solid lubrication of silicon nitride rolling elements, expertise with solid lubricated rolling element bearings at temperatures and speeds of interest to turbine designers is practically nonexistent. Taylor and coauthors [4] demonstrated that properly designed low speed bearings could function at 1000°F (540°C) and 1500°F (815°C). These bearing tests were conducted in protective nitrogen and argon atmosphere which is not considered practical for most applications.

Boes [5] has shown that titanium shrouded WSe_2-In-Ga composite cages were operable at speeds less than 30,000 rpm. Rapid composite wear resulted in excessive transfer film build up on the races and balls causing a loss of bearing internal clearance and bearing seizure.

Dayton, Sheets, and Shrand [6] investigated a slotted inner ring concept to assist in cooling the inner ring of a solid lubricated 7204 bearing. Their investigation revealed that at high speed cage unbalance was a considerable problem, and that bearing operating speed had the most significant effect on bearing temperature. Due to the cage unbalance, the effectiveness in cooling the bearing by a slotted inner ring could not be determined.

Recently, Nypan [7] nas tested a 61906 angular contact bearing to 47,000 rpm using a MoS_2 sputter coating on the bearing

surfaces. His investigation showed that the ball-cage pocket forces were approximately 9 lbf (40 N). No information was given on the test time at 47,000 rpm prior to failure of the lightly loaded bearing.

1.2 Program Objectives

The objective of this program was to investigate cage designs suitable for use with Pure Carbon P2003 graphite for high speed 7205 angular contact ball bearings. The test condition goals for the program were 55,000 rpm at a 100 lbf (450 N) thrust load at ambient temperature conditions.

1.3 Program Approach

Due to cage, bearing, and test complexity resulting from scale-up from solid lubricated four ball tests to solid lubricated full scale high speed angular contact bearings, the program "Solid Lubricated Silicon Nitride Bearings at High Speed and Temperature - Phase I," utilized a hybrid bearing to demonstrate the capability of the solid lubricant/cage system. The hybrid bearing consists of M50 steel rings, silicon nitride balls, and a cage containing solid lubricant. The hybrid bearing was evaluated using three different cage designs without the use of liquid lubricants at ambient temperature conditions to a maximum speed of 55,000 rpm. A specially designed test rig consisting of an air turbine drive, bearing housing, and load system was used to simultaneously test two solid lubricated bearings.

Analysis of the Phase I test results will yield advanced solid lubricated silicon nitride bearing design concepts. The present test system will be modified for the evaluation of solid lubricated silicon nitride bearings at 1000°F (540°C) at 55,000 rpm (5760 rad/sec) with a 100 lbf (450 N) thrust load. These bearings will be evaulated during the program "Solid Lubricated Silicon Nitride Bearings at High Speed and Temperature - Phase II." Figure 1 presents a flow chart containing the major tasks in Phases I and II.

2.0 Program Overview

At the initiation of the program "Solid Lubrication of Silicon Nitride Bearings at High Speed and Temperature - Phase I," it was believed that the investigation of various cage designs for solid lubricated hybrid ball bearings would yield valuable information on the bearing behavior without oil lubrication. Two basic cage designs were selected; a segmented 3 piece graphite cage and a stainless steel shrouded graphite cage. Although the behavior of the Pure Carbon P2003 at high temperature in rolling contact between M50 and silicon nitride had been

Figure 1 Logic Chart for "Solid Lubricated Silicon Nitride Bearings at High Speed and Temperature, Phases I and II"

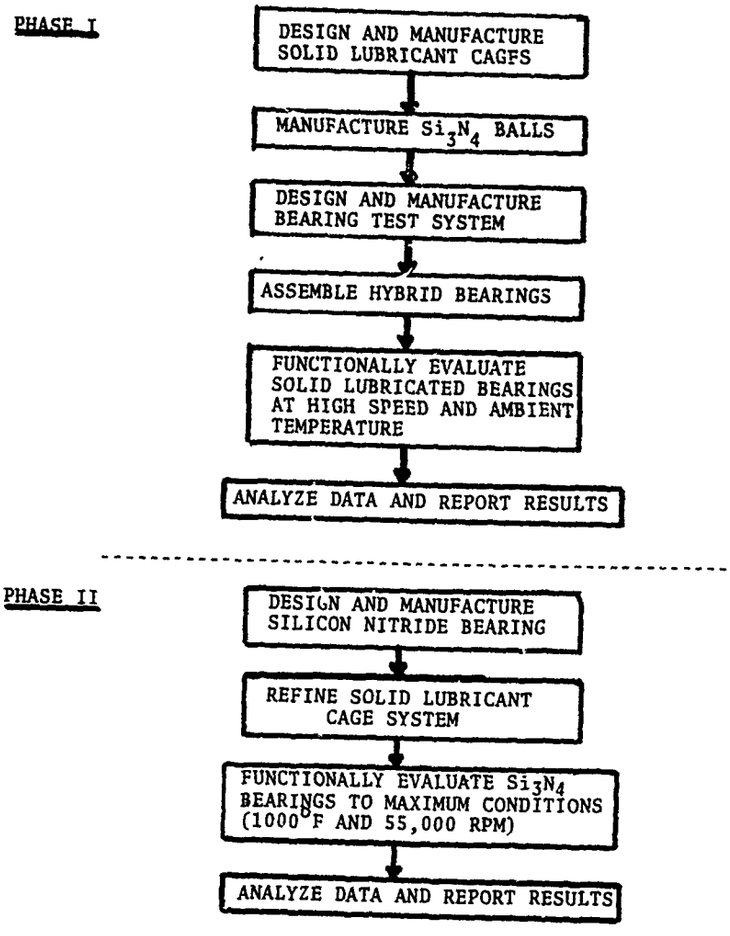

F-4185C-1-R100

demonstrated previously [3], the heat generation rate, cage wear, and cage unbalance at high speed in a rolling contact bearing were virtually unknown.

The first tests with a segmented cage indicated two requirements for successful operation of the outer land riding cage concept. First of all, the bearing land surfaces must be smooth to prevent rapid cage wear. In addition, bearing diametral clearances must be significantly increased compared to oil lubricated bearings to avoid bearing seizure. The bearing internal geometry must also be designed to tolerate a decrease in clearance due to the solid lubricant build-up and thermal expansion of the inner ring.

Additional evaluation of the segmented cage concept utilizing an increased bearing diametral clearance, .003 in (75 μm), revealed that the temperature differential between the inner and outer ring increased with increasing speed. Operation of the solid lubricated bearings was limited to approximately 25,000 rpm (2600 rad/sec). Increasing the speed resulted in bearing seizure since the Δ T between the rings exceeded 250°F (120°C). This Δ T was measured during the tests and verified by calculations utilizing the bearing clearance and thermal expansion coefficients of each bearing component.

A significant difference in the change of diametral clearance with bearing material was realized when comparing M50 steel properties to silicon nitride. For the hybrid bearing investigated, a ΔT of 250°F between the inner and outer ring will precipitate failure resulting from a loss in clearance and the corresponding large increase in contact stress. A silicon nitride bearing was predicted to tolerate ΔT's greater than 500°F (260°C) without difficulty as shown in Figure 2. The low thermal expansion coefficient of silicon nitride should have a major impact on solid lubricated bearing performance at high speed.

One other major point was observed during testing of the segmented cages. Extending the cage rail beyond the bearing envelope was detrimental. Unsupported sections of the cage can result in a flexural stress resulting in circumferential cracking through the cage web. Predictions of heat generation at high speed also indicated that a light weight fully supported segmented cage has a lower heat generation rate than heavier segmented cages.

Evaluation of a shrouded graphite cage confirmed the work of other investigators [6]. Unlike the segmented cage which is piloted by the outer land and groove, obtaining stability in a stainless steel shrouded cage will require considerable design expertise. Guidance and dampening of a shrouded cage is difficult since the cage contacts the ring at one location. De-

Figure 2 Effect of Thermal Gradients on Bearing Contact Angle and Contact Stress for Hybrid and Silicon Nitride Angular Contact Bearings

(Predicted using 0.003 in. [75 um] diametral clearance)

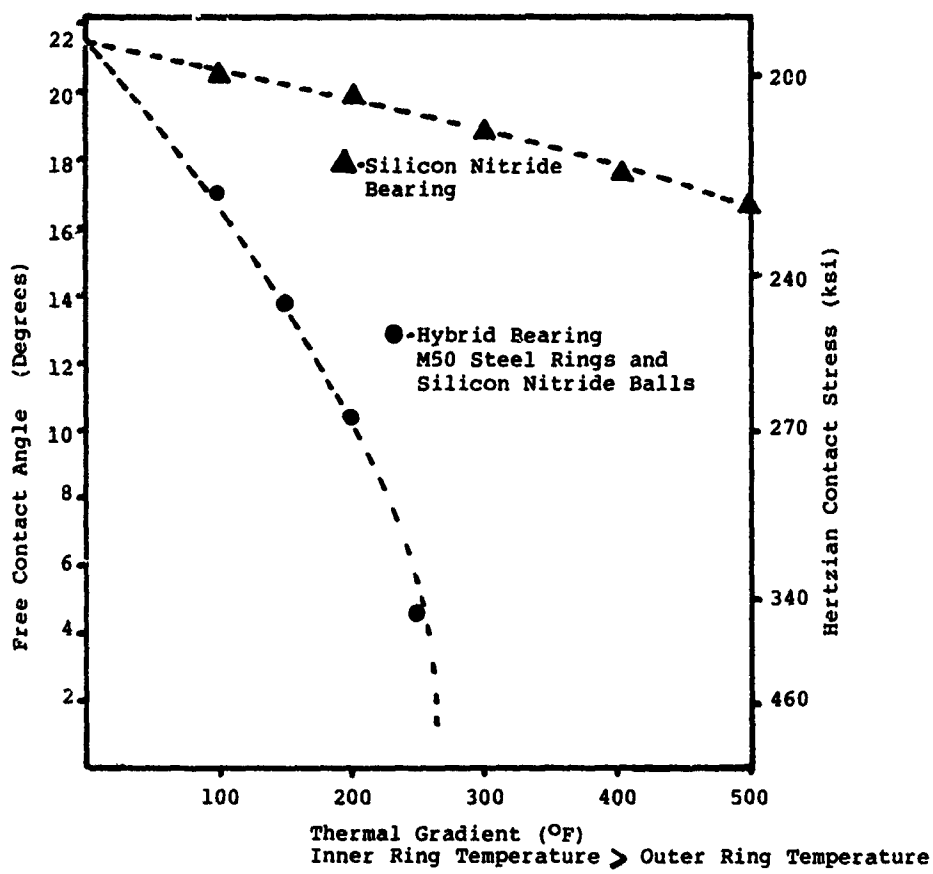

F-4185C-1-R100

creasing ball-pocket clearance may result in improved cage stability with an increase in heat generation.

In summary, the design of a high speed solid lubricated bearing is a difficult task which requires expertise in design, thermal modelling, and materials. Evaluation of the Phase I test results has shown potential for solid lubricated silicon nitride bearings. Development of a successful solid lubricated bearing for high speed applications will require proper selection of the bearing internal geometry, cage design, solid lubricant, and bearing mounting system.

3.0 Component Design, Manufacture, Inspection and Assembly

3.1 Component Design

3.1.1 Bearing Design

A 7205 type hybrid bearing comprised of nine silicon nitride balls, an M50 steel outer ring, an M50 steel inner ring, and a graphite containing cage was selected for evaluation. 6205 VFX aircraft quality M50 rings were modified to an angular contact hybrid bearing by grinding the appropriate bearing lands and replacing the M50 steel balls with silicon nitride balls. Figures 3 and 4 depict the modifications to the bearing lands necessary for bearing assembly with the solid lubricant cages. The rings shown in Figure 3 were used with the outer land riding cages, while ring modifications presented in Figure 4 were used with the inner land riding cages.

The 7205 bearing internal geometry contained in Table 1 was analyzed at two speed conditions using an SKF SHABERTH computer program modified for solid lubrication and the elastic properties of the silicon nitride rolling elements. As can be seen in Table 2, this analysis predicts an adequate bearing life and realistic Hertzian contact stresses for the bearing design and test conditions selected. The heat generation rate at 55,000 rpm (5760 rad/sec) resulted in concern due to the possibility of decreasing the bearing diametral clearance. A thermal mass model of the high speed bearing test rig drawing No. L-81108 was prepared to determine the effects of the heat generation rate on the bearing internal clearance.

By using the thermal mass model of the high speed test rig, a steady state inner ring temperature was calculated assuming three different friction coefficients for graphite transfer films in the Hertzian contact zone. The friction coefficients chosen (μ_f = 0.05, μ_f = 0.10, and μ_f = .15) were believed to bracket the friction coefficient for Pure Carbon P2003 transfer films at a 200 ksi (1450 MPa) contact stress. As may be seen in Table 3, the inner ring temperature ranged from 525°F (274°C) to 833°F (445°C) depending on the friction coefficient. The relatively

Figure 3 Bearing Envelope Used with Outer Land Riding Cages

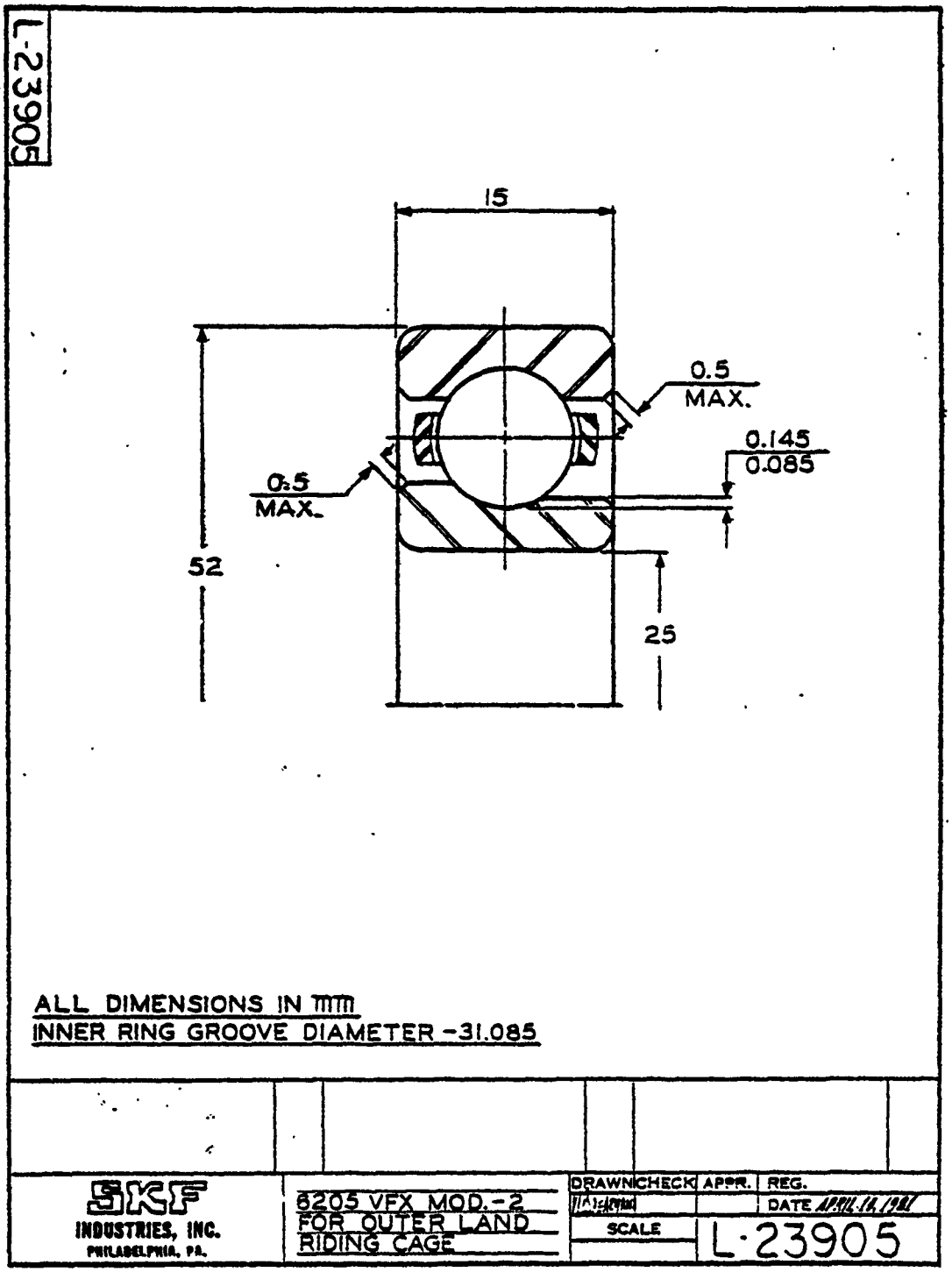

F-4185C-1-R100

Figure 4 Bearing Envelope Used with Inner Land Riding Cages

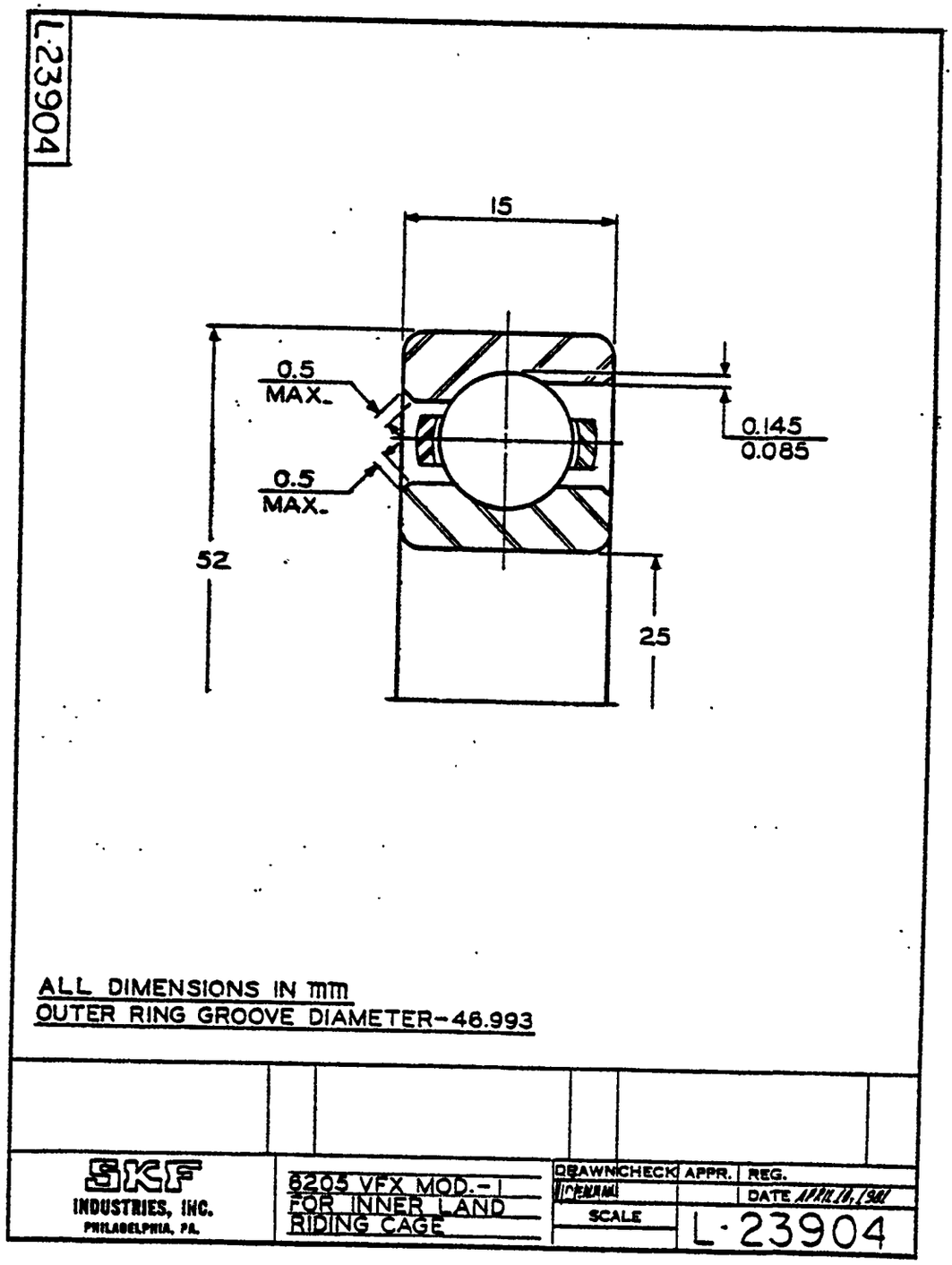

F-4185C-1-R100

Table 1 - Hybrid Bearing Design Evaluated by SHABERTH Computer Program

Ball Diameter:	7.9375 mm (0.3125 inch)
Ball Complement:	9
Contact Angle:	25°
Pitch Diameter:	39.040 mm (1.536 inch)
Diametral Clearance:	0.031 mm (0.0012 inch)
Groove Radius:	4.1275 mm (0.1625 inch) - inner
	4.143 mm (0.1631 inch) - outer
Conformity:	.52 - inner and outer

Table 2 - SHABERTH Computer Program Output for 7205 Bearing Containing Silicon Nitride Balls and Solid Lubricated

	Output	
	Case 1	Case 2
Shaft Speed	10,000 RPM (1050 rad/sec)	55,000 RPM (5760 rad/sec)
Thrust Load	100 lbf (450 N)	100 lbf (450 N)
Cage Speed	4070 RPM (425 rad/sec)	22,950 RPM (2400 rad/sec)
Contact Angle		
Inner Race	23°	29°
Outer Race	23°	15°
Hertzian Contact Stress		
Inner Race	220 ksi (1540 MPa)	210 ksi (1450 MPa)
Outer Race	185 ksi (1280 MPa)	210 ksi (1450 MPa)
Heat Generation Rate:	μ_f = 0.05 10 watts	60 watts
	μ_f = 0.15 ----	170 watts
Bearing L10 Life	3200 hours	750 hours

Table 3 - NAVAIR Solid Lubricated 7205 Hybrid Bearing Steady State Operating Temperatures, No Cooling Air Supplied to Bearing

Shaft Speed (rpm)	μ_f	Temperatures				
		Shaft °F (°C)	Inner Ring °F (°C)	Ball °F (°C)	Outer Ring °F (°C)	Housing °F (°C)
55,000	0.05	527 (275)	525 (274)	495 (257)	453 (234)	441 (227)
55,000	0.10	675 (357)	680 (360)	635 (335)	568 (298)	550 (288)
55,000	0.15	822 (439)	833 (445)	775 (413)	684 (362)	660 (349)
10,000	0.10	417 (214)	413 (212)	392 (200)	358 (181)	351 (177)
10,000	0.15	433 (223)	430 (221)	406 (208)	369 (187)	361 (183)

high predicted bearing temperatures are due to frictional heat generation and the low thermal conductivity of the stainless steel test rig (17$\frac{4}{}$ PH stainless).

Since the predicted inner ring temperature at the maximum temperature 833°F (445°C) was close to the maximum safe operating temperature of the M50 bearing steel, an analysis of the effect of cooling air on bearing temperature was conducted for the bearing-test rig system. Figure 5 shows that adding 4 cubic feet of air per minute to the test rig will reduce the inner ring maximum temperature to 500°F (260°C), which was well within the capability of M50 bearing steel.

One other potential problem area was investigated, that of reduced bearing clearance due to inner ring thermal expansion. The bearing clearance was calculated using the results of the SHABERTH program presented in Table 3. With a M50 bearing, steel balls and rings, a net loss of clearance would result for all three cases investigated. For the hybrid bearing, it was determined that the bearing clearance increases due to the thermal expansion of the bearing outer ring, which has a 63% larger mean diameter than the inner ring. Since the inner ring temperature > ball temperature > outer ring temperature, this temperature profile normally results in a net loss in bearing clearance. The low thermal expansion coefficient of the Si_3N_4 ball resulted in a net gain in bearing clearance for a bearing operating at the temperatures predicted in Table 3.

3.1.2 Cage Design Guidelines

The solid lubricant/cage systems selected for evaluation at high speed in 7205 angular contact hybrid bearings are the result of literature review and conversations with experts in the field. Review of the literature [8, 9, 10, 11, 12] revealed very little information pertaining to the solid lubrication of rolling contact bearings at high speed and temperature. Most knowledge of cage design concepts has been restricted to oil lubricated gyro-type bearings. Instabilities in the bearing/cage system for gyro bearings can result in large spacecraft point errors. Therefore, computer simulation of gyro bearing cage systems have been used to predict the dimensional tolerances required for stable gyro-cage operation.

No proven models or experience exists for a high speed solid lubricated bearing system. Also, in a solid lubricated bearing, the cage must play a dual role. The cage must supply lubricant and act as a ball separator.

The review of oil lubricated cage design, information on solid lubricant cages, and results from the NAVAIR Program [3] provided guidelines for the solid lubricant cage design.

Figure 5 Predicted Bearing Temperature as a Function of Air Flow Rate through Test Rig Design L-81108

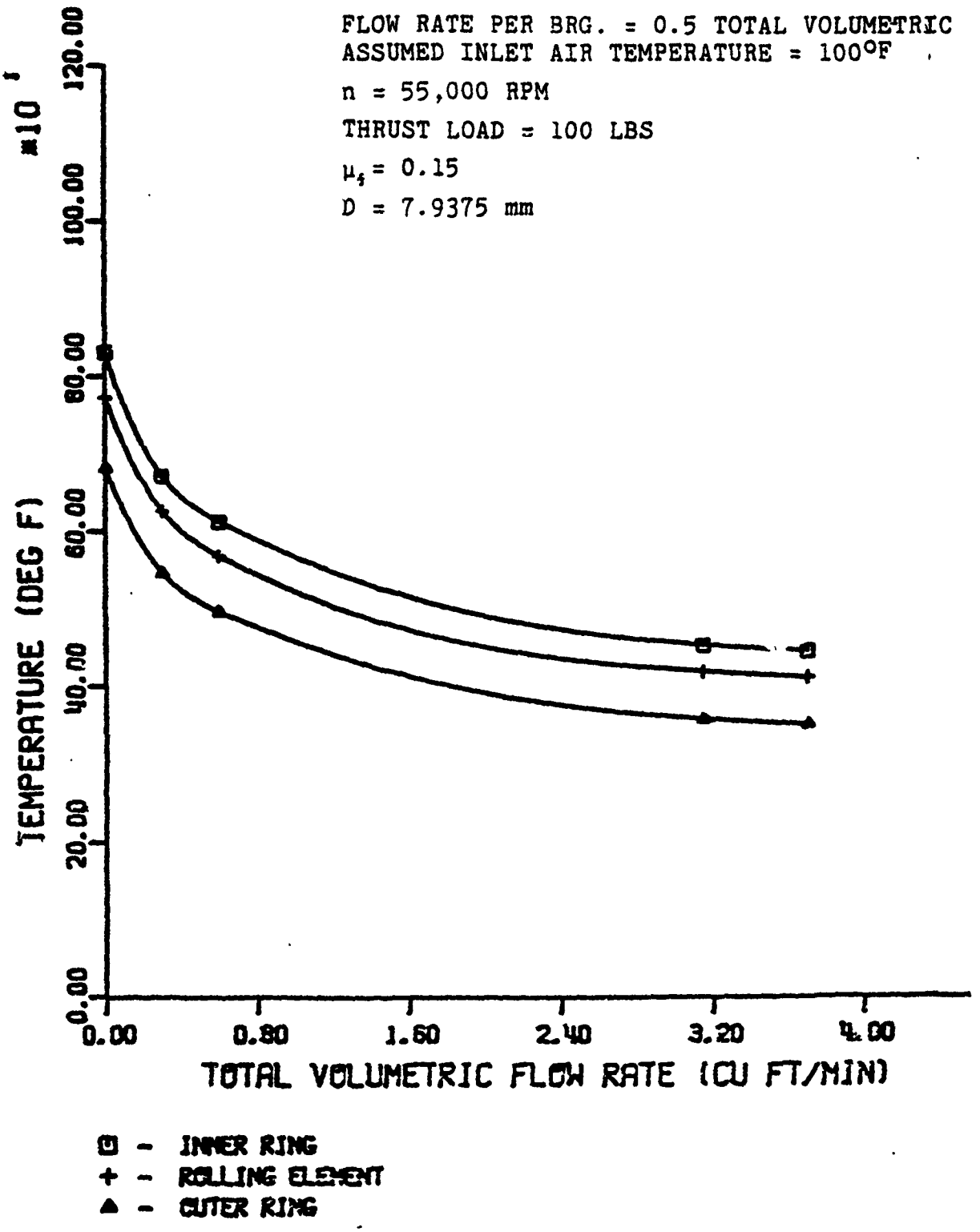

F-4185C-1-R100

The general guidelines for solid lubricant cage design based on oil lubricated cage studies were as follows:

1. Ball pocket clearance should be greater than cage to land clearance.

2. Cage material should have a low density.

3. High speed bearings should have outer land guided cages, if possible.

The cage design guidelines from the NAVAIR program

1. Material must be an effective solid lubricant (P2003 graphite chosen).

2. Ball-cage contact surface should be initially non-conforming to allow initial rapid cage wear for rapid solid lubricant transfer.

Based on the literature review [8, 9, 10, 11, 12] and conversations with other investigators in the field of solid lubrication, three cage designs were selected for evaluation in the 7205 angular contact bearing. Figures 6 and 7 show outer land riding segmented graphite cage concepts. In Figure 6, the graphite segments are completely constrained by the outer ring of the bearing. The hoop tensile stress normally associated with a high speed cage is minimized by segmenting the cage. The major stresses experienced by this cage include ball loading at the cage pockets, flexure stress due to bending of the segments, and impact loading at the ends of the cage segments. Axial stability of the cage segments is obtained by using the outer ring groove to pilot each segment. Stress calculations had indicated that the cage design shown in Figure 6 could fracture due to bending of the cage segments. Therefore, the cage design utilizing an extended cage rail was developed, Figure 7.

A conventional inner land riding cage design was also selected for evaluation. Figure 8 shows the drawings of the 174 PH stainless steel/graphite cage. In this design, the possibility of graphite fracture was reduced by placing the graphite in compression. Based on the thermal expansion of 174 PH and the Pure Carbon P2003 graphite, an 0.008 in (0.20 mm) interference fit was used to maintain the interference at a 1000°F (540°C) test temperature. The shrouded graphite cages were evaluated in the bearing design shown in Figure 4.

Figure 6 Graphite Segmented Cage Design L-23845

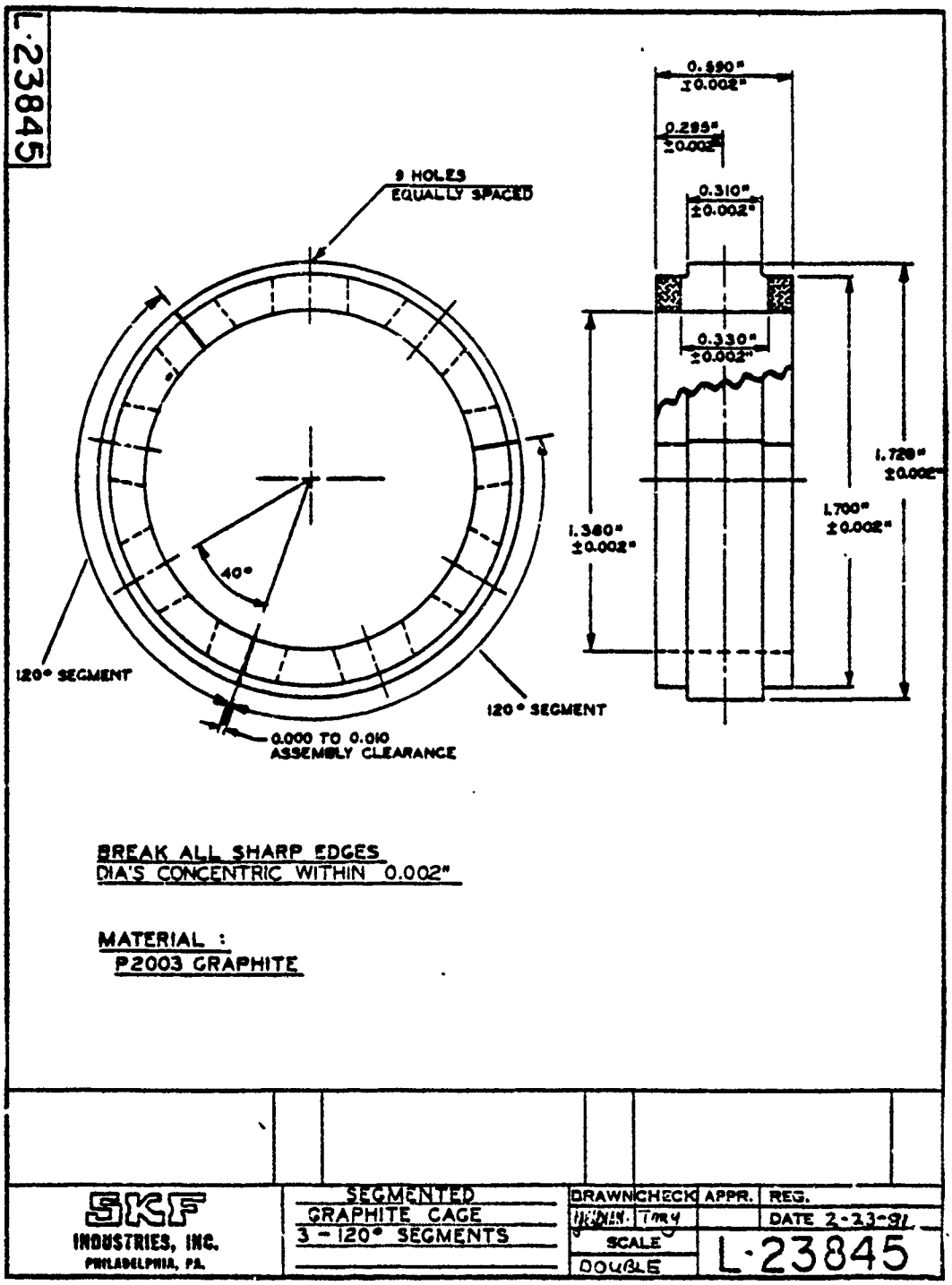

F-4185C-1-R100

Figure 7 Graphite Segmented Cage Design L-23875 with Cage Rail Extending Beyond Bearing Envelope

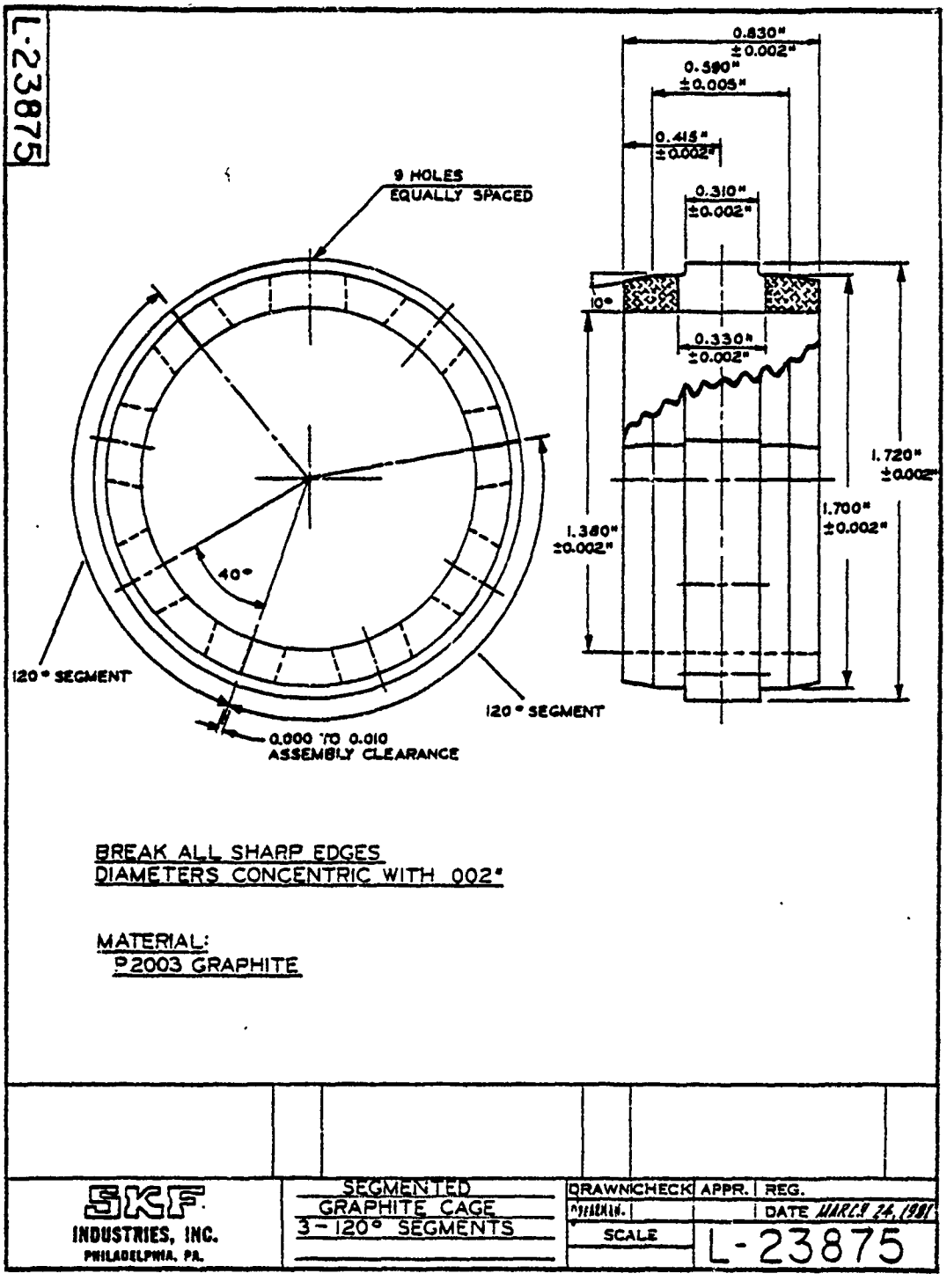

F-4185C-1-R100

Figure 8 Stainless Steel Shrouded Graphite Cage

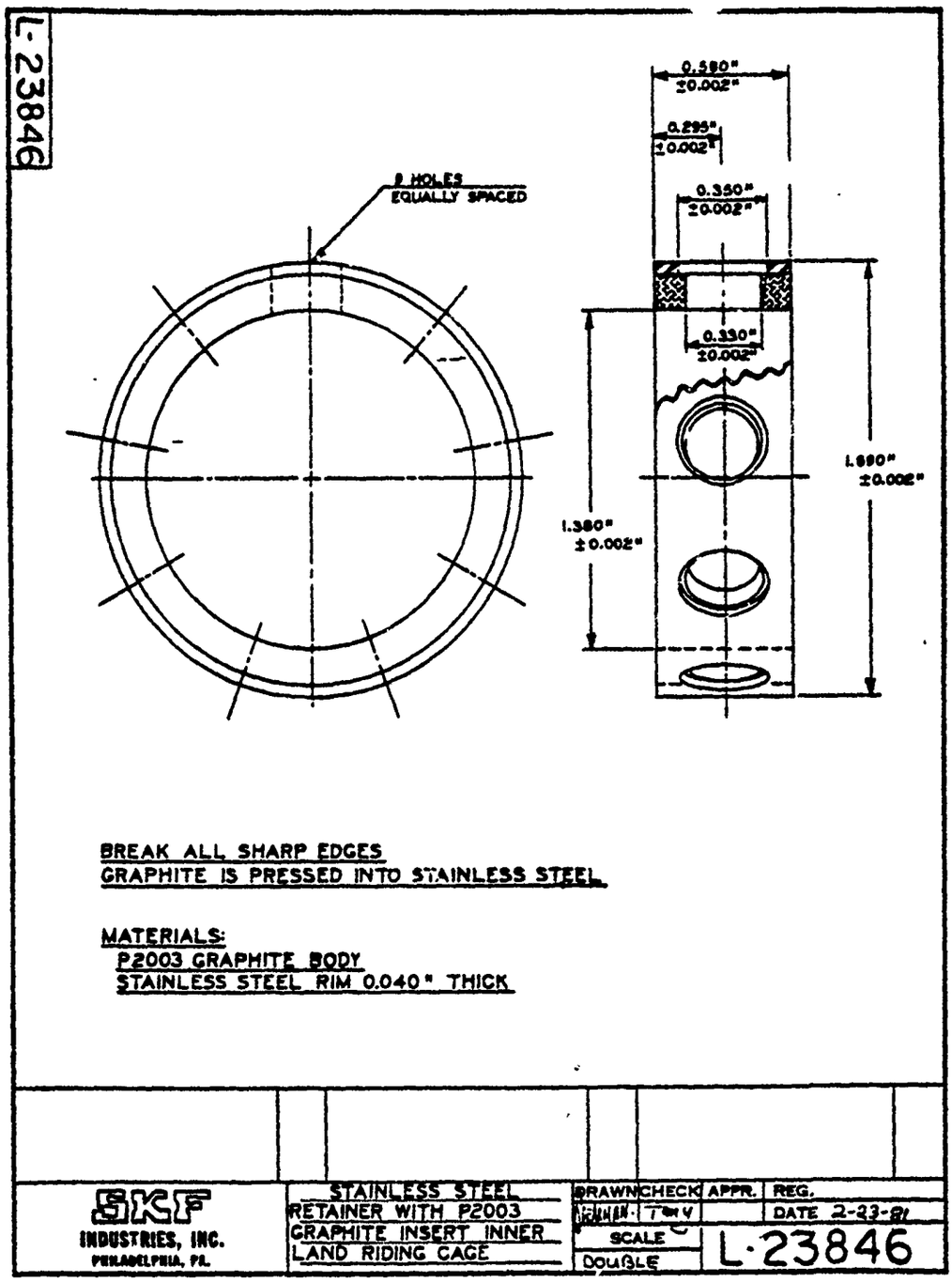

F-4185C-1-R100

3.2 Manufacture and Inspection

3.2.1 Silicon Nitride Balls

3.2.1.1 Material

The ceramic material used for the manufacture of the 0.313 in (7.95 mm) balls and purchased for Phase II ring manufacture was Norton NC132 hot pressed silicon nitride (HPSN) obtained from the Norton Company. Quality control procedures were implemented in the areas of raw material inspection as well as non-destructive evaluation of the finished parts to assure production of the highest quality silicon nitride balls.

The Norton certification data and SKF certification indicated that the silicon nitride utilized in ball manufacture was comparable to that used in previous programs [2, 3].

3.2.1.2 Dimensional Quality

The 160 silicon nitride balls produced during this program conformed to AFBMA grade 10 roundness requirements. Grade 10 balls have a maximum allowable 2 point out of roundness of 10 x 10^{-6} in (0.25 μm). Surface roughness was approximately 1 x 10^{-6} in AA (0.02 μm AA). Sufficient ball quantities were produced in Phase I to allow completion of all scheduled tests for "Solid Lubricated Silicon Nitride Bearings at High Speed and Temperature - Phases I and II.

3.2.1.3 Non-Destructive Evaluation

The silicon nitride balls were subjected to a 100% fluorescent dye penetrant inspection. A sensitive fluorescent dye penetrant (Zyglo ZL-30; ZR-10A) was used to impregnate the balls at Peabody Testing/Magnaflux. Visual inspection was conducted using ultraviolet light. No material related defects were observed by this technique.

Inspection of the ball surface by scanning electron microscopy did not detect any evidence of inter connected porosity or other deleterious conditions.

3.2.2 M50 Steel Rings

Existing SKF 6205 VFX M50 steel rings were converted to the 7205 angular contact bearing by grinding the appropriate bearing land. The measured groove radius was 0.163 in (4.142 mm) on the inner ring and 0.167 in (4.23 mm) on the outer ring.

3.2.3 Graphite Containing Cages

The segmented cage designs, SKF drawing numbers L-23845 and

L-23875, shown in Figures 6 and 7, were purchased from Pure Carbon Co. Five cages of each design were obtained from Pure Carbon Co. The graphite used as the solid lubricant was Pure Carbon P2003 graphite which was shown to be effective at preventing silicon nitride wear and M50 steel wear at high temperatures [3].

The stainless steel shrouded graphite cage shown in Figure 8 was fabricated at SKF. Four 174PH stainless steel rings were finished to the dimensions shown in Figure 9. The graphite was then inserted into the stainless steel shroud by heating the stainless steel ring to approximately 1200°F. The room temperature graphite ring was then forced into the shroud. After allowing the assembly to cool to room temperature, the ball pockets were drilled through the graphite. The inner diameter was then machined to the drawing requirements. Figure 10 depicts three 174PH stainless steel shrouded cages to SKF drawing L-23846.

3.3 Bearing Assembly

The bearing rings and silicon nitride balls were ultrasonically cleaned in acetone prior to assembly. The bearing outer rings were then heated to approximately 400°F (200°C) to facilitate assembly. Figure 11 shows the cages and assembled bearings.

4.0 Experimental Procedure

4.1 Test Equipment

A bearing test rig with high temperature capability was designed and fabricated for this program. The bearing test system shown in Figures 12, 13, and 14 was designed to test two solid lubricated bearings simultaneously. No additional support bearings were required in the high temperature test rig. The test bearings were axially loaded by a calibrated load beam through a load plug and the shaft.

The bearing test rig was coupled to an existing SKF Barbour-Stockwell No. 1658 air turbine. This air turbine has a speed capability in excess of 55,000 rpm (5760 rad/sec).

The 174 PH stainless steel bearing housing contained heaters capable of 1000°F (540°C) operation for extended periods of time. The cartridge heaters were circumferentially spaced in the bearing housing.

Since computer analysis had indicated that cooling air would be beneficial, filtered cooling air was supplied to the bearing cavity. The cooling air flow rate could be controlled from 4 SCFM to 12 SCFM. The cooling air flow was not directed at the bearing inner ring. However, the rig design required the air flow to pass through the inner and outer rings of both test bearings.

Figure 9 174PH Stainless Steel Shroud and Graphite Insert Used in Cage Design L-23846

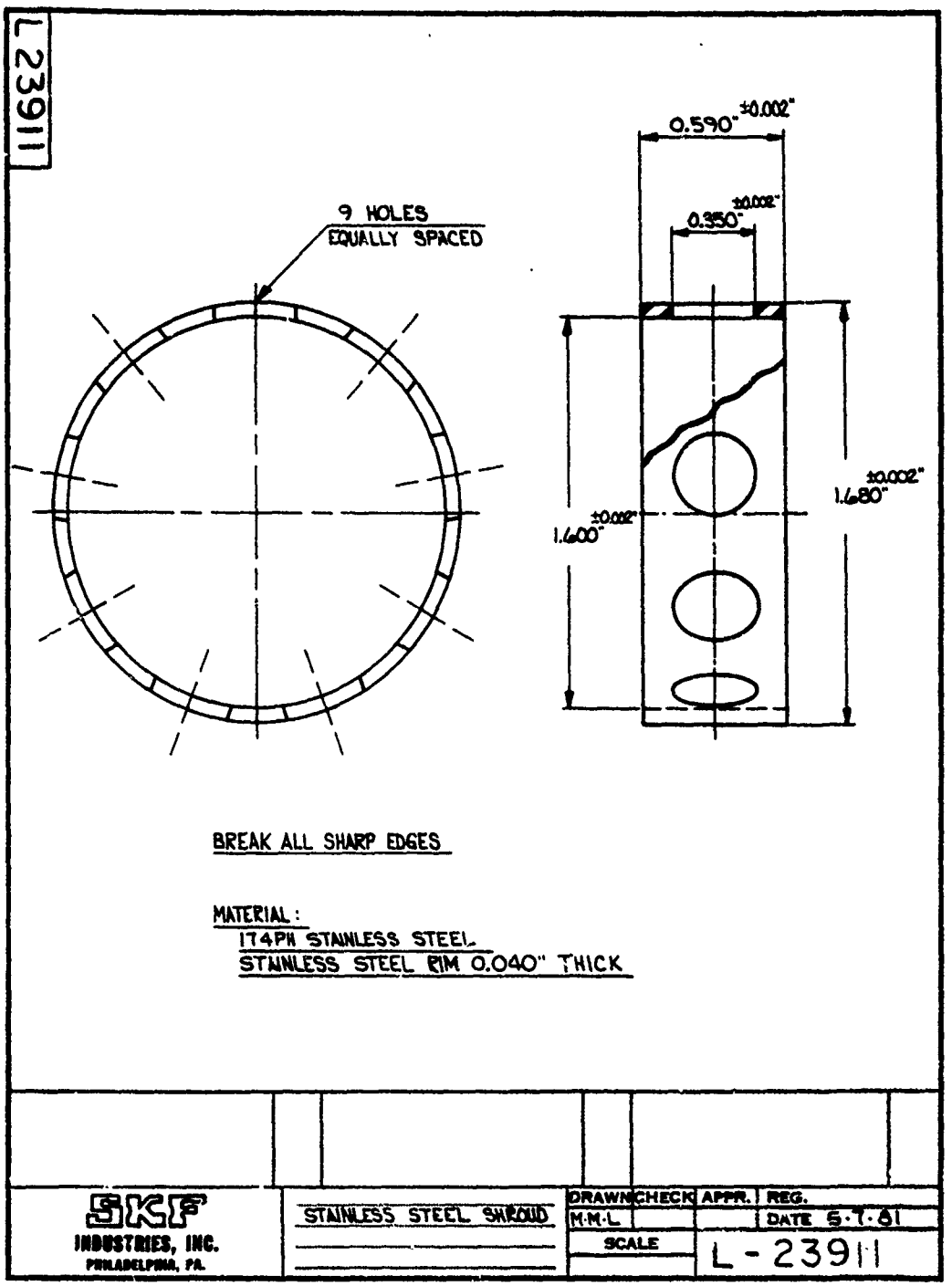

F-4185C-1-R100

Figure 9 (continued)

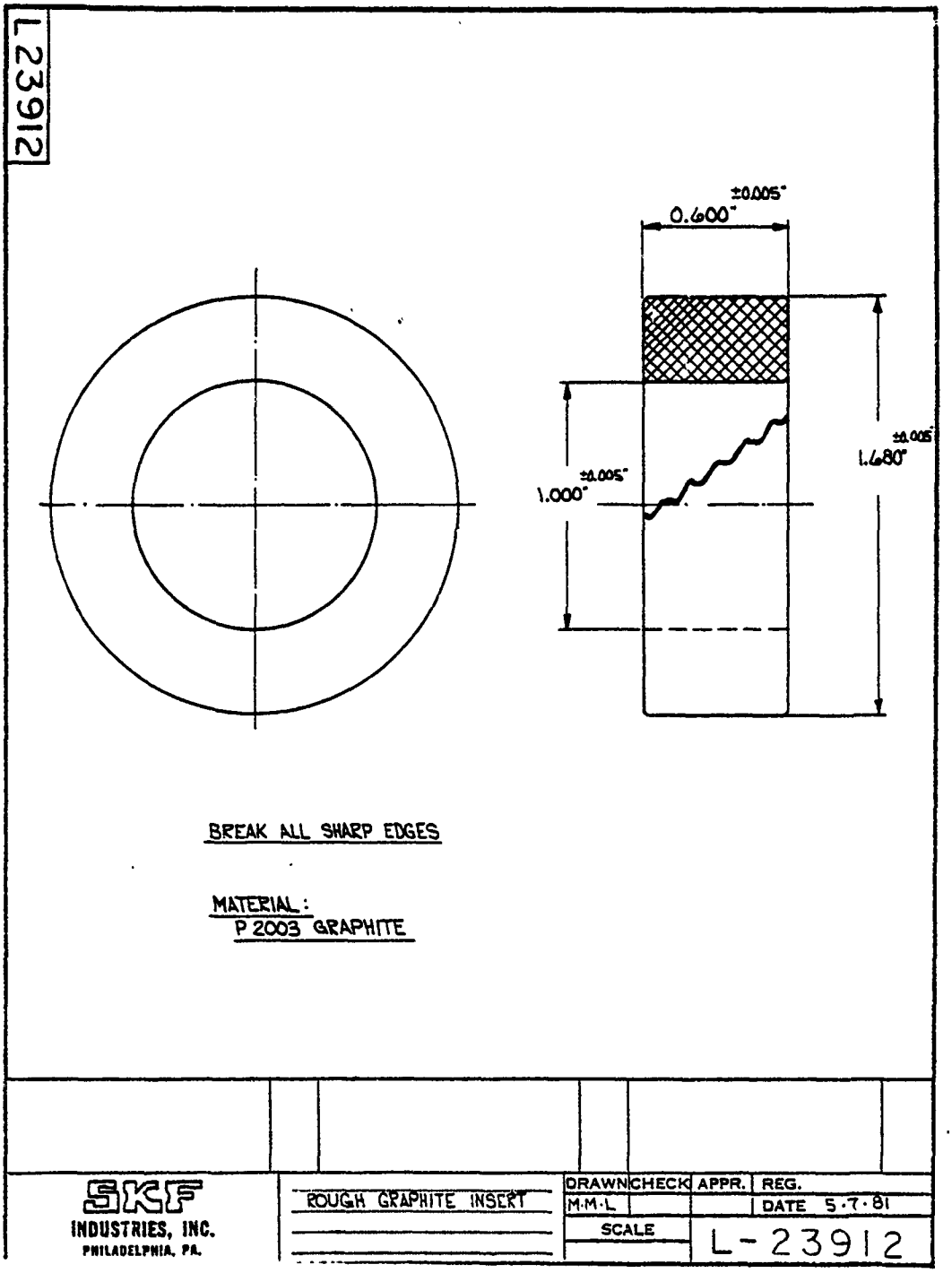

F-4185C-1

Figure 10 Photograph of Finished Shrouded Cages

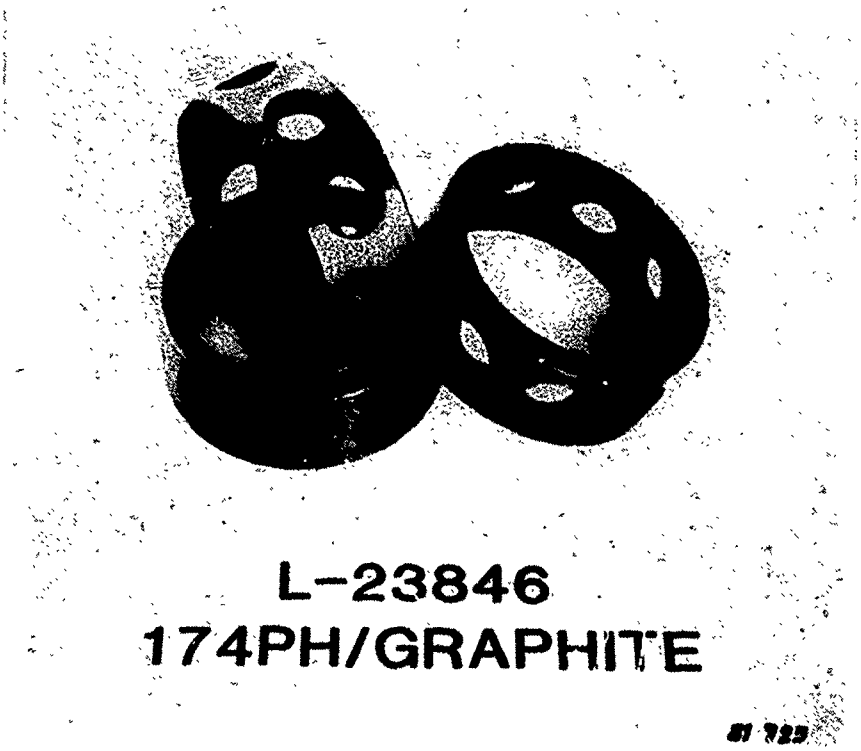

Figure 11 Photograph of Cage Designs L-23845, L-23846, and L-23875

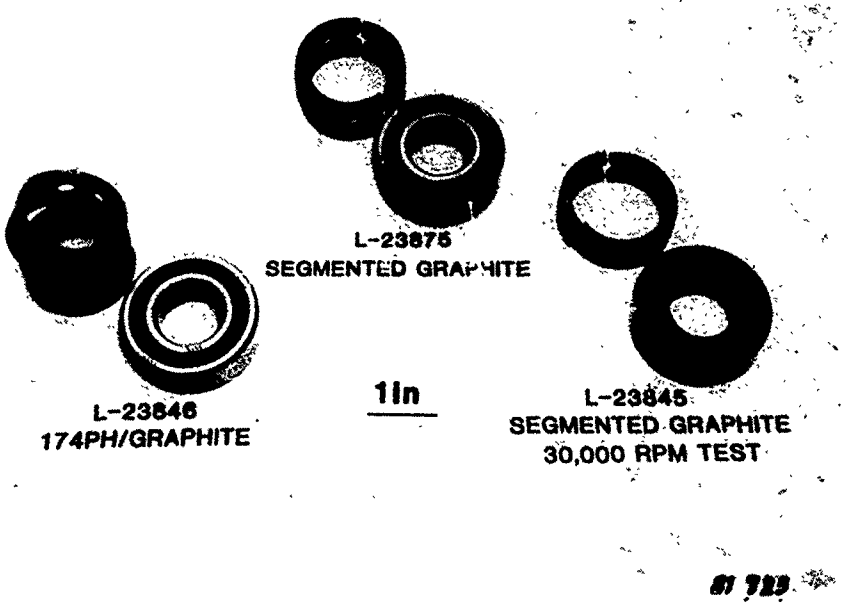

F-4185C-1-R100

AT82D002

Figure 12 - Overall View of Bearing Test Rig Design L-81108

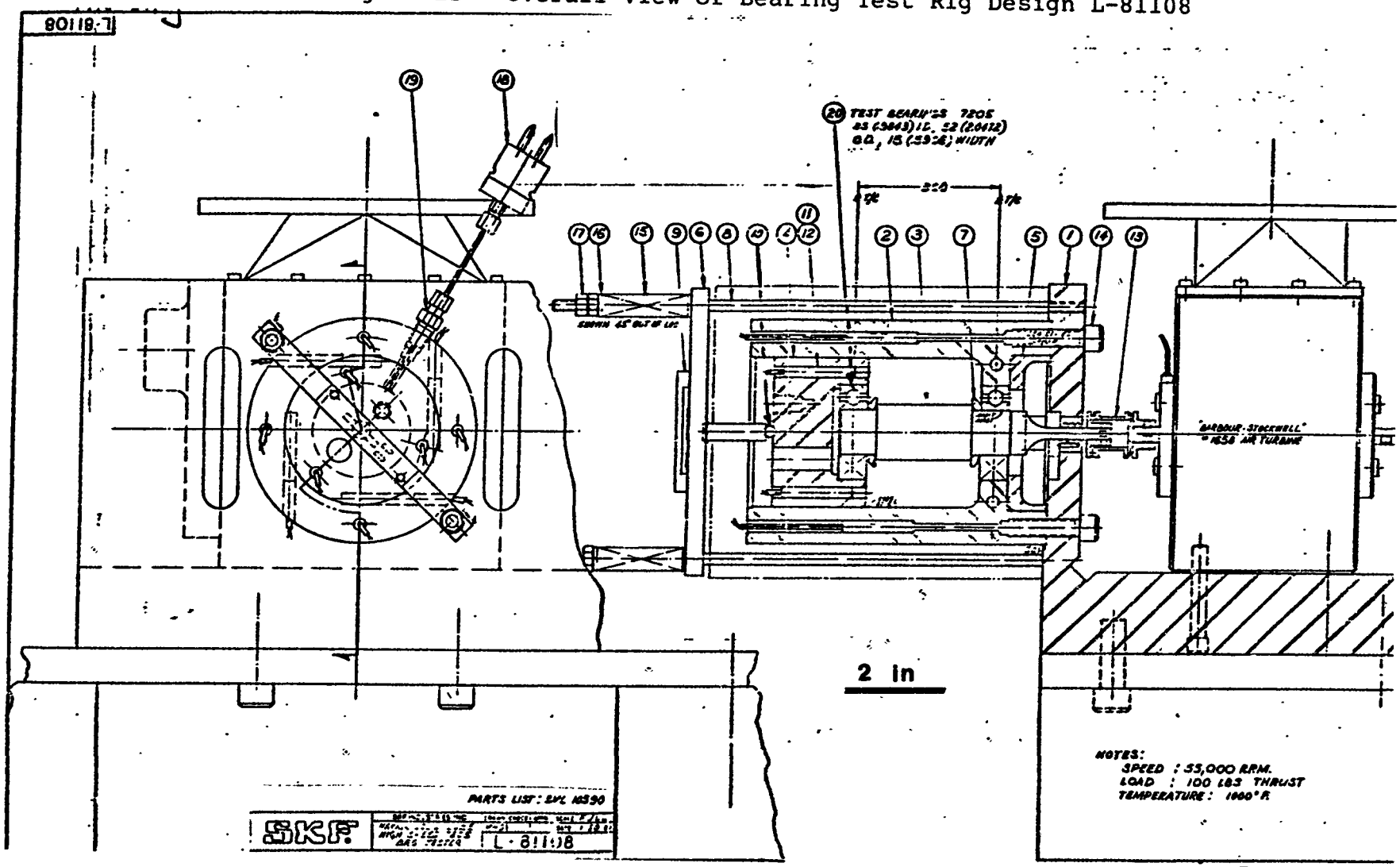

AT82D002

Figure 13 - Side View of Test Rig L-81108

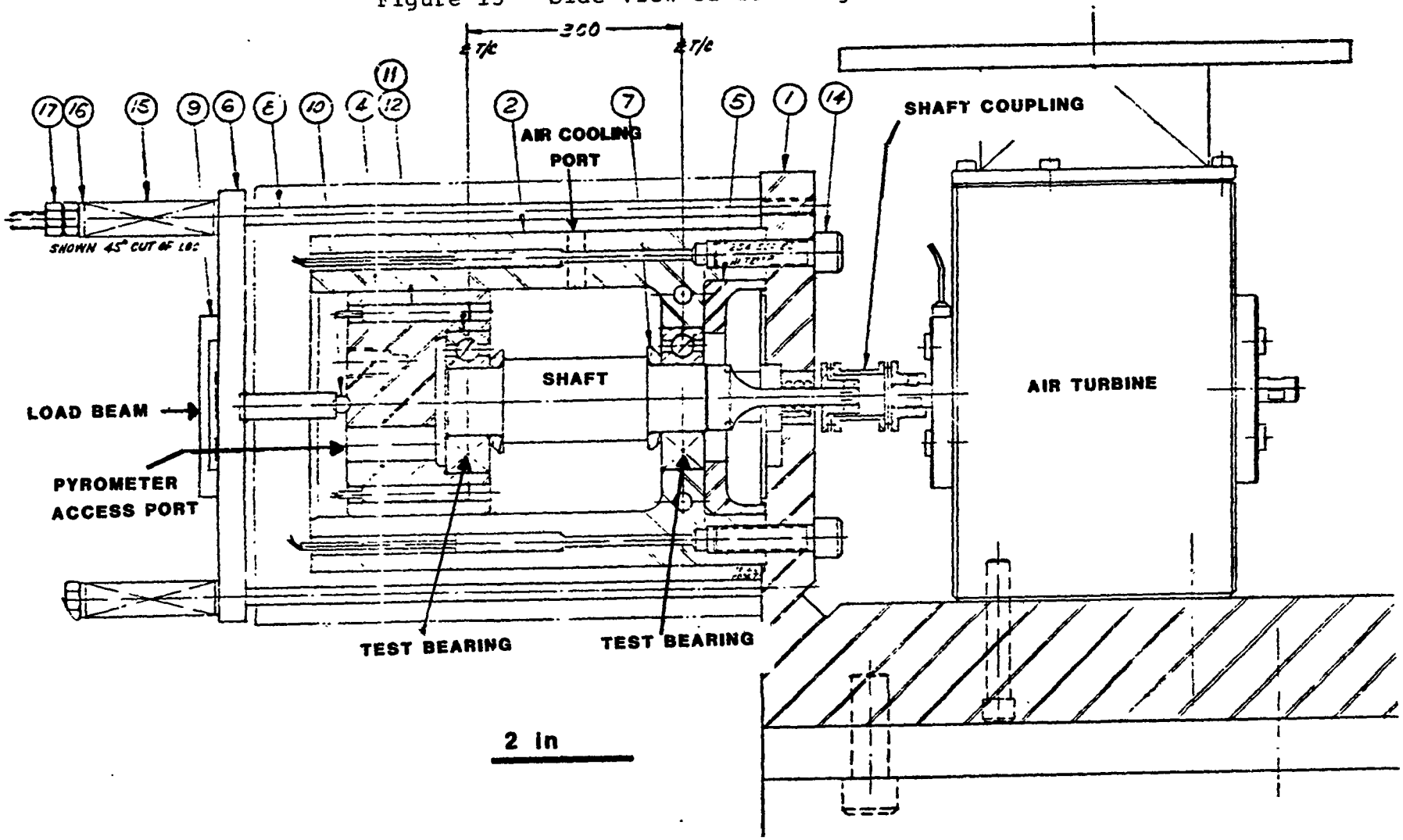

Figure 14 End View of Test Rig L-81108

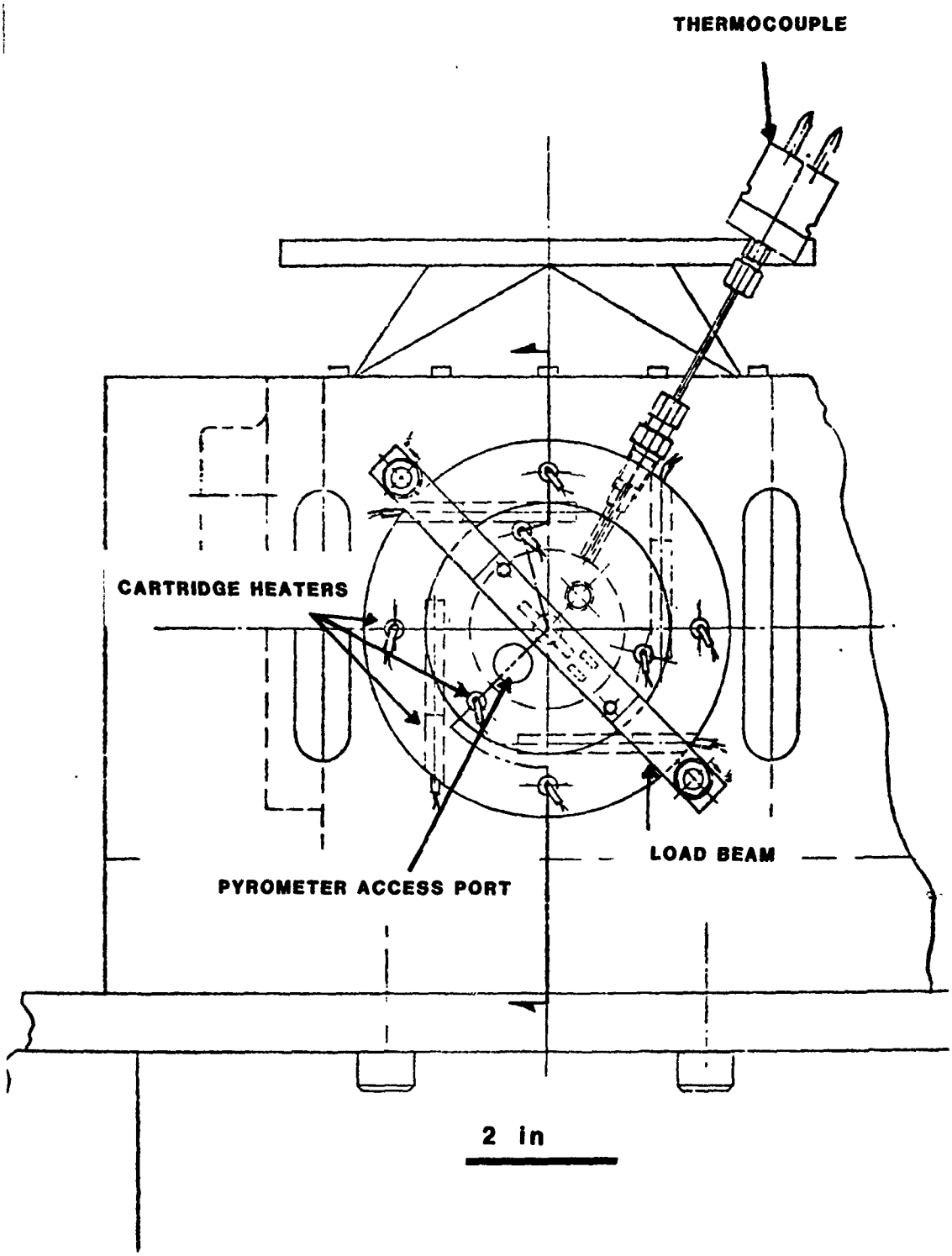

F-4185C-1-R100

Bearing outer ring, load plug, and housing temperatures were determined by iron-constantan thermocouples. The bearing inner ring temperature for the bearing contained within the load plug was determined using an Ircon infrared pyrometer. A one half inch diameter (13 mm) access port through the load plug was directed at the bearing inner ring as shown in Figures 13 and 14.

Turbine speed was determined using a magnetic pickup system supplied with the air turbine. Inlet air pressure to the turbine and speed was controlled manually through series of air valves.

4.2 Test Procedure

The 7205 bearings were retained in a desiccator until test evaluation. The three piece cage design L-23845 was evaluated first, followed by the cage designs L-23875 and L-23846.

To initiate a test, two solid lubricated bearings containing the same cage design were pressed onto each end of the 174PH shaft. The measured interference was approximately 0.0007 inches (0.018 mm) which reduced the bearing internal clearance by 0.0005 inches (0.013 mm). After pressing the bearings on the shaft, the load plug was inserted over the load plug bearing. This completed assembly was then slipped into the bearing housing. Once the bearings were properly seated in the housing, the load was applied through the load plug by a calibrated load beam. The thermocouples and heaters were connected to the proper recording channels and controllers. Ceramic fiber insulation was used to minimize the anticipated temperature gradients between the inner and outer rings. The test bearing shaft was coupled to the drive system by a flexible connector.

Cooling air was supplied to the test bearing cavity at approximately 4 SCFM. The tests were conducted by slowly increasing the turbine speed by a manually controlled air valve. The test procedure selected was to increase the speed 10,000 rpm (1050 rad/sec) after bearing temperatures had stabilized.

Bearing temperatures, speeds, and general observations were recorded on a data sheet for each test.

4.3 Inspection

The tested bearings were examined by low power optical microscopy, optical microscopy, and scanning electron microscopy with an attached x-ray wavelength analyzer. A sensitive three point gauging instrument capable of detecting 0.00001 in (0.25 µm) was used to determine the ball diameter before and after the tests.

5.0 Results and Discussion

5.1 Introduction

Appendix A presents a sequential listing of the high speed bearing test summaries. The following subsections present the results and discussion for the bearing cage designs evaluated during the course of this program.

5.2 Oil Mist Lubricated Bearings

The purpose of the tests with oil lubricated bearings was to verify air turbine performance, control response, bearing alignment, and load distribution. The test rig check out runs were conducted using standard 52100 steel 7205 C/P4 DGA bearings in the bearing housing. For these tests oil mist lubrication was supplied to the bearing cavity through the air cooling port in the housing. The first set of 7205 C/P4 DGA bearings was functionally evaluated to a maximum speed of 50,000 rpm (5760 rad/sec). Slight speed variations were noted throughout the test. However, by increasing the oil mist supply to the test bearings from 10 psi to 17 psi it was possible to decrease the magnitude of the speed variation. A total of 32 minutes of test time was achieved at a shaft speed above 40,000 rpm (4200 rad/sec).

Inspection of the test bearings revealed that the bearings were poorly lubricated. Evaluation of the wear track on the bearing rings revealed the possibility of an incorrect load application.

A second test was conducted using two new 7205 C/P4 DGA bearings with the oil mist pressure increased to the bearing cavity. Approximately 13 minutes of test time was conducted above 45,000 rpm (4700 rad/sec). A total test time of 4 minutes was realized at 55,000 rpm (5760 rad/sec) prior to an increase in bearing temperature and bearing seizure. Inspection of these bearings confirmed that bearings were properly loaded and that insufficient oil lubrication had precipitated failure. Since this series of tests had indicated the proper application of load and 55,000 rpm turbine capability, testing with solid lubricated 7205 bearings was initiated.

5.3 Solid Lubricated Hybrid Bearings Utilizing a Segmented Graphite Cage - Intital Tests

The first solid lubricated 7205 angular contact bearing tests were conducted using a three piece segmented graphite cage, SKF Drawing Number L-23845, for both test bearings. The unmounted bearing diametral clearance was 0.0012 in (31 μm). The bearing inner ring - shaft interference fit used resulted in a

reduction of the mounted diametral clearance to approximately 0.0007 in (18 μm). Therefore, the bearing housing temperature was increased to 200°F (93°C) in an effort to preferentially expand the bearing outer ring, thereby increasing the bearing diametral clearance. Unfortunately, the temperatures measured by thermocouples located at the inner and outer rings of the stationary bearings revealed that the inner and outer ring temperatures were identical. Bearing diametral clearance could not be increased by heating the bearing housing.

The first solid lubricated bearings were evaluated with a 0.0007 in (18 μm) clearance and the segmented graphite cage design L-23845. A 100 lbf (450 N) axial load was applied to the test bearings, then the bearing housing temperature was allowed to stabilize at 200°F (93°C). Cooling air was supplied to the bearing cavity at 4 SCFM for this test.

To initiate the test, the air valve to the air turbine was opened manually. The turbine speed was increased to 10,000 rpm (1050 rad/sec) and held at that speed until the bearing temperature had stabilized. The bearing temperature stabilized at 230°F (110°C) after approximately 2 minutes of test. The bearing inner temperature was less than 350°F (175°C), the lower limit of the Ircon Infrared Pyrometer. Some cycling of the turbine speed was noted, but believed to be relatively insignificant due to the low torque capability of the air turbine at 10,000 rpm. Increasing the turbine speed to 20,000 rpm (2100 rad/sec) resulted in an outer ring temperature of 390°F (200°C) and a 400°F (205°C) inner ring temperature. Further increases in test speed, 30,000 rpm (3150 rad/sec) resulted in bearing seizure. The maximum inner ring temperature observed was 600°F (315°C), while the outer ring temperature was beyond the recorder range of 390°F (200°C). The observed temperature differential between the inner ring and outer ring prior to bearing seizure was greater than the calculated 85°F (30°C) necessary to reduce the bearing diametral clearance to zero.

Inspection of the bearings revealed that the segmented cages for both bearings were in excellent condition even though the bearings had seized. Figure 15 shows the bearings after the 30,000 rpm test. The silicon nitride balls were evenly coated with the graphite transfer film as can be seen in Figure 15. Figure 16 presents the cage pocket wear marks and the piloting wear marks. The cage which had been sliding against a rougher bearing land had a larger wear area, as shown in the photographs in Figure 16.

The initial test conducted with two solid lubricated bearings was encouraging due to the visually acceptable cage wear and graphite transfer films on the bearing surfaces.

AT82D002

Figure 15 - Photograph of Solid Lubricated Angular Contact Bearing after Test 1

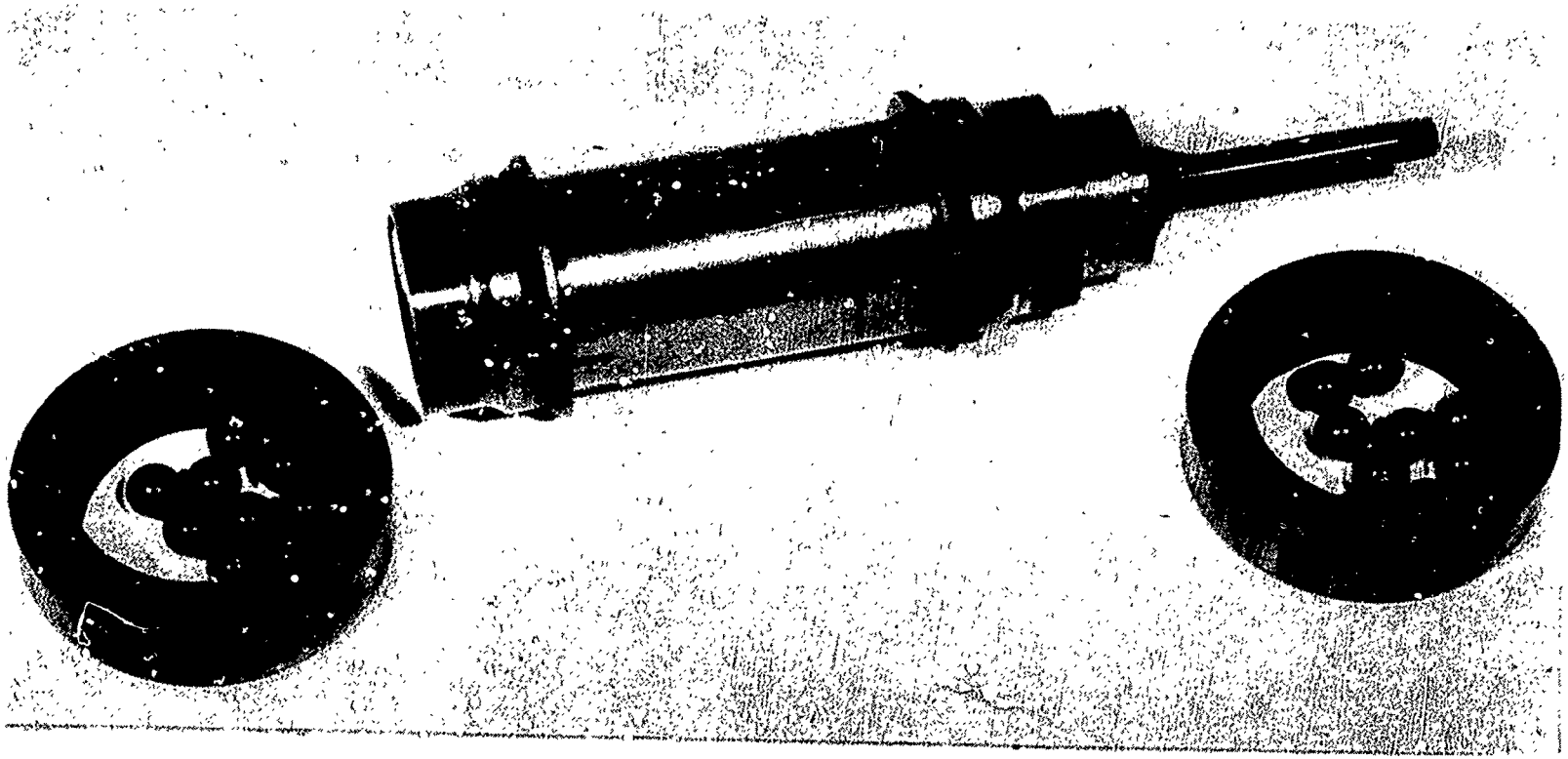

Figure 16 Cage Pocket Wear Marks and Piloting Wear Marks Observed on Segmented Cages

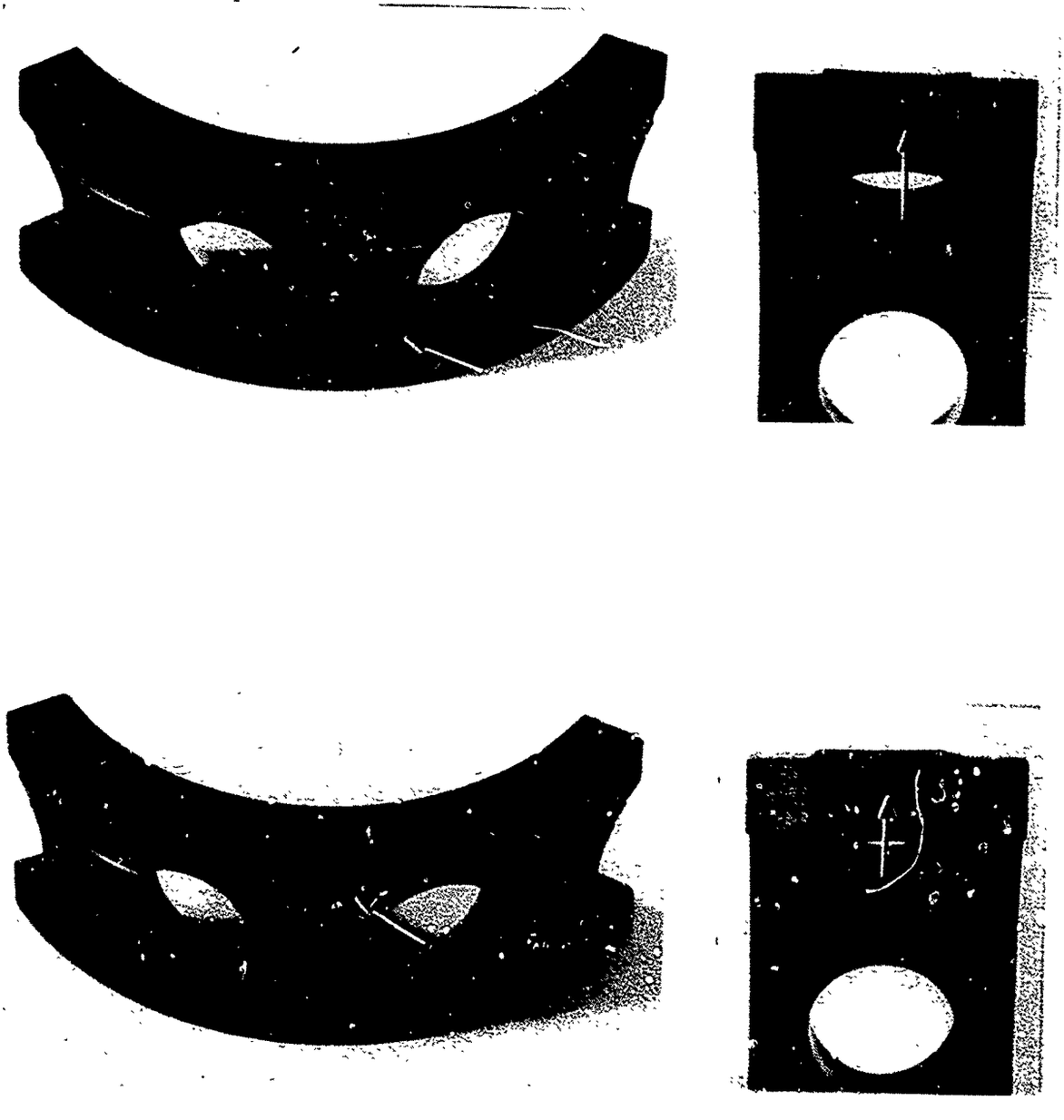

F-4185C-1-R100

A second series of tests was conducted at a 25 lbf (110 N) load with the bearings having a diametral clearance of 0.0007 in (18 μm). The segmented cage design L-23845 was used for these tests. In this test series, the outer ring land surface was ground to improve the surface finish. The purpose of this test series was to gain more experience with the behavior of high speed solid lubricated bearings and the test system.

The initial test of the second test series was test 2-1. In this test, the housing temperature was increased to 400°F (205°C) to allow the outer ring to expand. No improvement in bearing clearance was realized, since the inner ring and outer ring temperatures were identical. This bearing was evaluated by gradually increasing the turbine speed to a maximum of 32,000 rpm (3350 rad/sec). At 32,000 rpm the test bearings seized and the turbine air pressure was shut off.

Visual inspection of the test bearing through the optical pyrometer port in the bearing load plug revealed that the segmented cages had not failed. A second test in this series, test 2-2, was initiated with ambient housing temperatures. Increasing the bearing housing temperature was considered to be detrimental, since no improvement in bearing diametral clearance was realized and housing was not uniformly heated. Test 2-2 was conducted by slowly increasing the turbine shaft speed while the bearing housing was cooled with 4 SCFM of air. As can be seen in Figure 17, the bearing outer ring temperature continued to increase with increasing speed. At 40,000 rpm (4200 rad/sec), bearing seizure occurred. A maximum inner ring temperature of 450°F (230°C) and outer ring temperatures of 300°F (150°C) were observed prior to bearing seizure.

The results of tests 2-1, 2-2, and 2-3 indicated that bearing temperatures were considerably greater than predicted. In order to demonstrate the capability of a segmented cage design, three tests were conducted by rapidly accelerating the air turbine to 55,000 rpm (5760 rad/sec). Test 2-4, 2-5, and 2-6 demonstrated that the segmented cage design could survive accelerations to 55,000 rpm. Figure 18 presents the maximum inner ring and outer ring temperatures. Visual inspection of the segmented cage through the pyrometer port in the load plug after tests 2-4 and 2-5 indicated that the segments had survived the test. During test 2-6, the air turbine air pressure was inadvertently increased instead of decreased as planned. Bearing seizure at 55,000 rpm (5760 rad/sec) resulted in fracture of the segmented cage as well as damage to the silicon nitride balls. A detailed examination of the components was not conducted, since the test was not considered representative.

Figure 17 Test Speed versus Recorded Temperature for Test 2-2

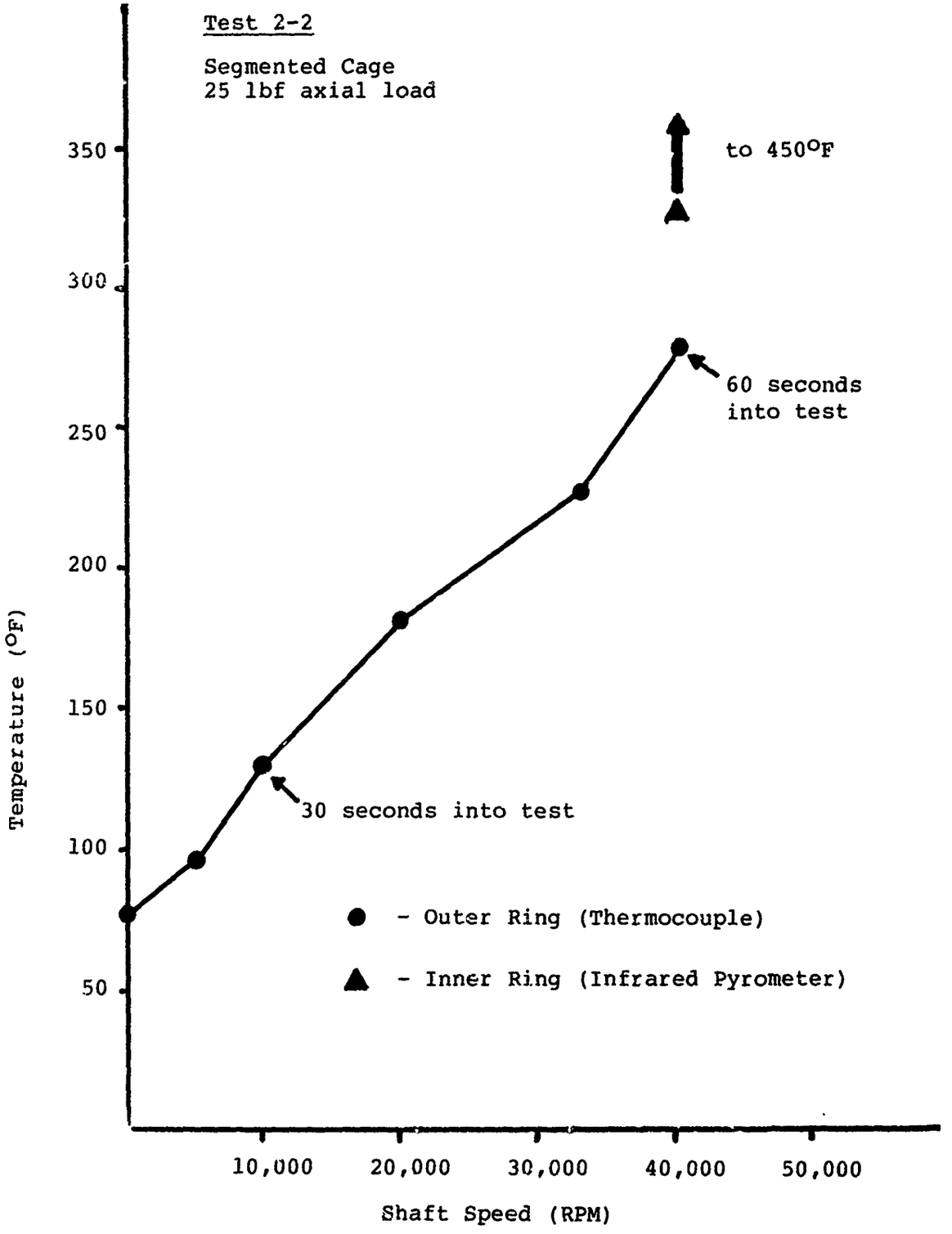

F-4185C-1-R100

Figure 18 Inner Ring and Outer Ring Temperatures Observed During Tests 2-4, 2-5, and 2-6

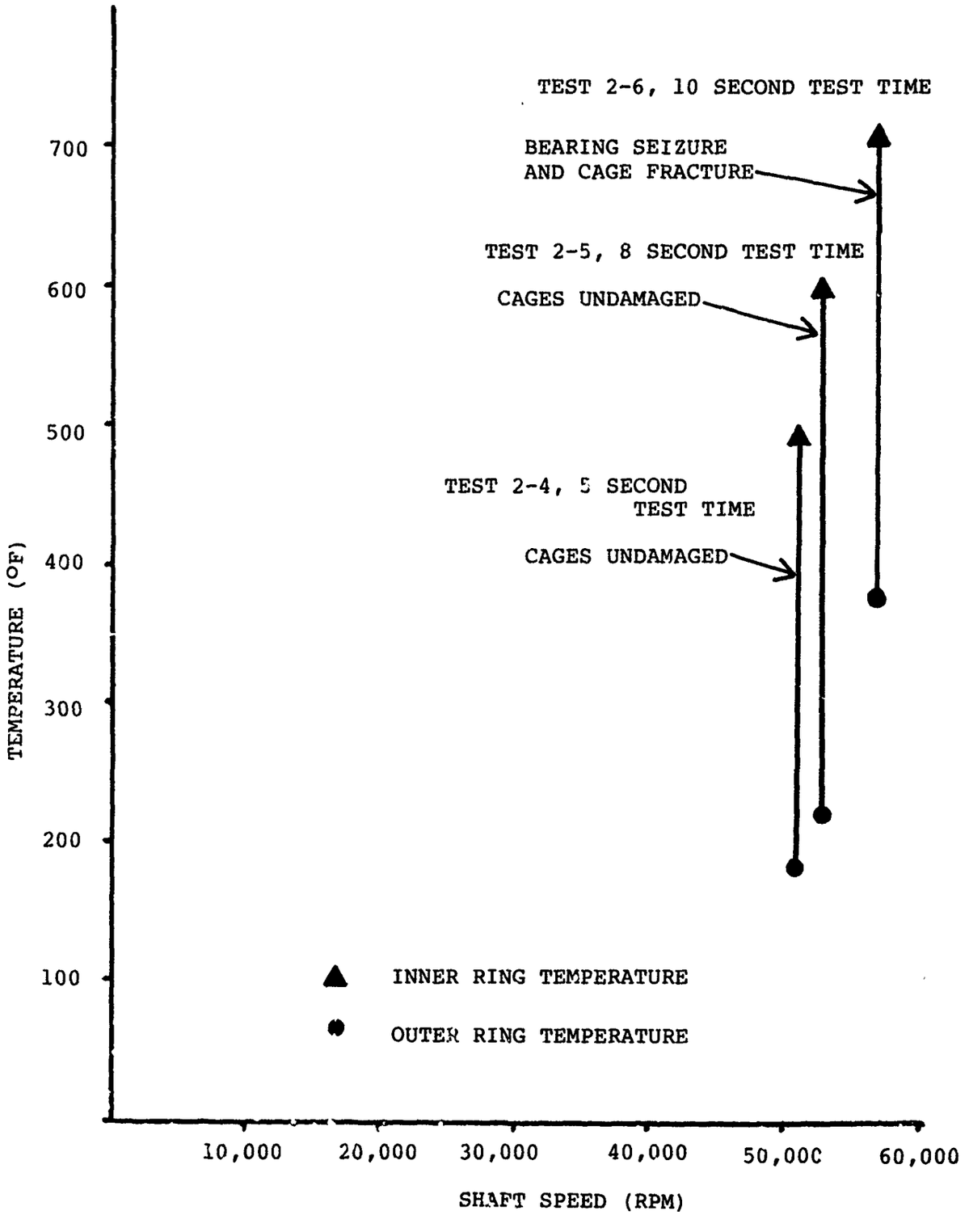

5.4 Evaluation of Solid Lubricated Angular Contact Bearings

5.4.1 Introduction

The initial tests with a solid lubricated angular contact bearing, section 5.3, disclosed that the computer predictions of bearing life and the thermal modelling did not completely describe the test system. In addition to the optimistic predictions of increased diametral clearance for a hybrid bearing, two other factors were believed to contribute to bearing failure:

1. Decreased bearing clearance due to interference fit.
2. Increased cage wear due to the surface roughness of the outer ring.

Additional tests with solid lubricated bearings containing segmented cages were conducted with increased diametral clearance and improved outer ring land surfaces.

The bearing diametral clearance was increased by reducing the silicon nitride ball diameter. Forty silicon nitride balls were decreased in diameter by lapping then polishing, to yield an unmounted bearing diametral clearance of 0.003 in (75 μm) with the existing rings. The surface roughness of the bearing lands was improved by grinding the lands and polishing.

Further evaluations of bearings containing segmented graphite cages were conducted using the increased diametral clearance and the polished bearing outer land surfaces.

5.4.2 Tests with Cage Design L-23875

The cage design L-23875, Figure 7, was evaluated in test numbers 3 and 4. In test number 3, the hybrid bearing had an increased diametral clearance, 0.003 in (75 μm). Two bearings were mounted on the shaft, the test system was assembled, and the test initiated at ambient temperature. The shaft speed was accelerated to 10,000 rpm (1050 rad/sec) and allowed to stabilize. After approximately 10 minutes, the outer ring temperature stabilized at 150°F (65°C). The inner ring temperature was below 350°F (175°C), the temperature limit of the infrared pyrometer. Accelerating the air turbine to 20,000 rpm (2100 rad/sec) resulted in an increase in the outer ring temperature to 250°F (120°C) and an inner ring temperature of 400°F (205°C).

Since the bearing diametral clearance was increased for this test series, another attempt at heating the housing to improve bearing performance was initiated. The bearing housing temperature was increased to 250°F (120°C) to match the outer ring

temperature experienced in the 20,000 rpm test with these bearings. The air turbine shaft was accelerated to 23,000 rpm which yielded a 550°F (290°C) inner ring temperature and a 400°F (205°C) outer ring temperature. An additional test to 33,000 rpm (3460 rad/sec) was conducted which resulted in bearing seizure. The maximum temperatures observed were 750°F (400°C) and 425°F (220°C) on the inner and outer rings, respectively. Figure 19 shows the components used in this test series. As can be seen, one segmented section was fractured. Visual inspection of the other segmented sections disclosed a circumferential crack pattern in another segment. The circumferential crack pattern through the cage segment was believed to be related to flexure of the unsupported portions of the cage. The flexure of the cage would place a bending movement on the cage webs and eventual fracture.

Test series 4 was conducted with two new cages of cage design L-23875. By gradually increasing speed, a series of tests to 25,000 rpm were completed. Bearing seizure continued to be a major problem even though the cooling air to the bearing cavity was increased from 4 SCFM to 12 SCFM. An attempt to accelerate the turbine to 55,000 rpm (5760 rad/sec) resulted in bearing seizure and extensive damage to the segmented cages.

5.4.3 Tests with Cage Designs L-23845 and L-23846

The 174PH stainless steel shrouded cage design, L-23846, was functionally evaluated in tests 5 through 8. In tests 5, 6, and 7, a segmented graphite cage of design L-23845 was used for the load plug bearing while the shrouded cage design was evaluated in the drive end portion of the bearing housing. This conservative test approach was selected due to the favorable test experience with the segmented cage design at low speed and the unknown response of an inner land riding shrouded graphite cage design.

Comparisons of the ball pocket wear marks in the two cage designs after test 5 disclosed that the segmented cage had transferred considerably more graphite lubricant to bearing surfaces than the shrouded cage under identical test conditions. Since test 5 was limited to 5,000 rpm (525 rad/sec) due to bearing noise, test 6 was conducted at a higher speed 10,000 rpm (1050 rad/sec) while disregarding any bearing noise or squeal. Although cage pocket wear was observed to be appreciable, a continuous graphite transfer film was not observed on the M50 steel ring surfaces. This observation indicated that the high air flow rate through the bearings, approximately 6 SCFM/bearing, was removing the graphite from the bearings. Considerable evidence of graphite particles down stream from the bearing confirmed that graphite particles were removed from the bearing by the high air flow rate.

AT82D002

Figure 19 Bearing Appearance After Bearing Seizure in Test 3

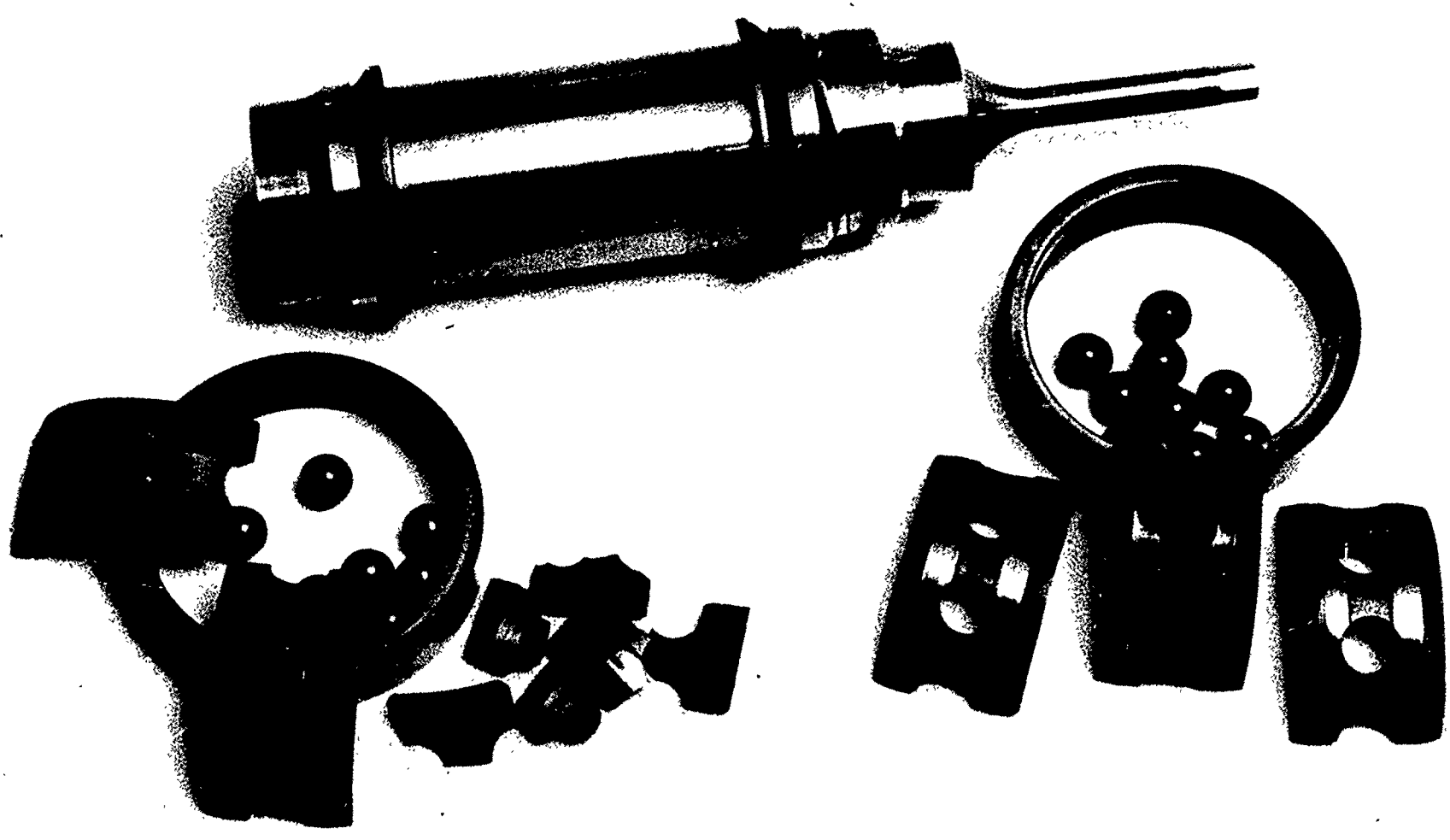

Test 7 was conducted to determine whether the air flow rate did affect the solid lubricated bearing performance. In this test, the air flow rate was reduced to zero SCFM from the 12 SCFM air flow rate used in test 6. Test 7 progressed smoothly with the same cages used in tests 5 and 6 to a maximum speed of 22,000 rpm (2300 rad/sec).

Thirty-three minutes into test 7, the bearings emitted a "squeal." Disassembly and inspection of the bearings revealed that a few silicon nitride balls had contacted the stainless steel shroud. As may be seen in Figure 20, the silicon nitride balls had contacted the entire cage pocket circumference indicating that the cage had moved axially throughout the entire 0.020 in. (0.5 mm) ball pocket clearance and the balls contacted the stainless steel shroud in a few locations.

In test 8, two shrouded graphite cages of design L-23846 were evaluated simultaneously without air cooling. Initiation of test 8 disclosed severe cage vibrations at low speed. Attempts to increase the bearing speed were unsuccessful due to vibration which threatened to destroy the solid lubricant containing cages. Inspection of these cages revealed a 360° wear track in the cage pocket. Inadequate axial guidance and the lack of cage dampening were considered to be the main causes of failure in test 8.

5.5 Discussion of Solid Lubricated Bearing Concepts

5.5.1 Introduction

The development and successful demonstration of a high speed, solid lubricated bearing requires the proper selection of bearing materials, lubrication systems, bearing monitoring systems, and bearing design. The previous program [3] demonstrated that acceptable silicon nitride wear rates could be achieved through the use of graphite transfer films. The most effective solid lubricant was Pure Carbon P2003 graphite based on analysis of the silicon nitride wear measurements. In the simplified four ball test system, used for investigations, the approximate bearing DN was an order of magnitude less than the 1.4 million DN at the 55,000 rpm (5760 rad/sec) goal for the program, "Solid Lubricated Silicon Nitride Bearings at High Speed and Temperature, Phase I." In addition, small changes in solid lubricated bearing contact angle, diametral clearance, and friction have considerably more influence on bearing performance that comparable changes in the rolling four ball test system. For example, a small decrease in diametral clearance due to thermal gradients or solid lubricant build-up results in a relatively insignificant change in the contact angle and stress in the four ball system. The spindle ball essentially "floats" on the three support balls which minimizes the effects of these changes. A similar small decrease in bear-

Figure 20 Graphite Cage Pockets in Shrouded Cage After Test 7 Showing Ball Contact at the Stainless Steel Shroud and Pocket Circumference

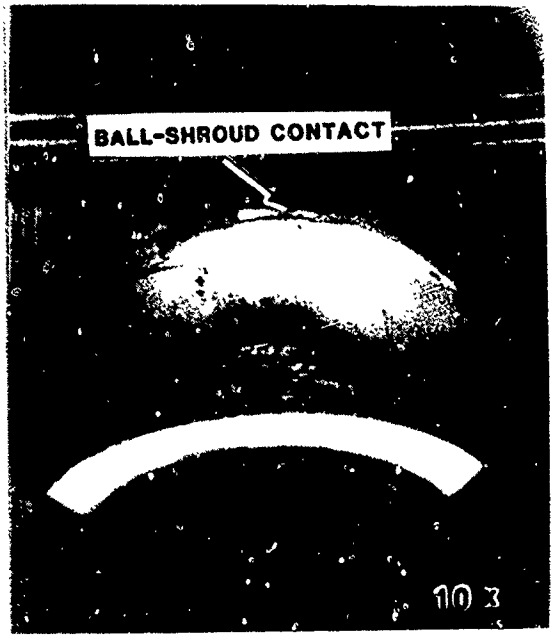

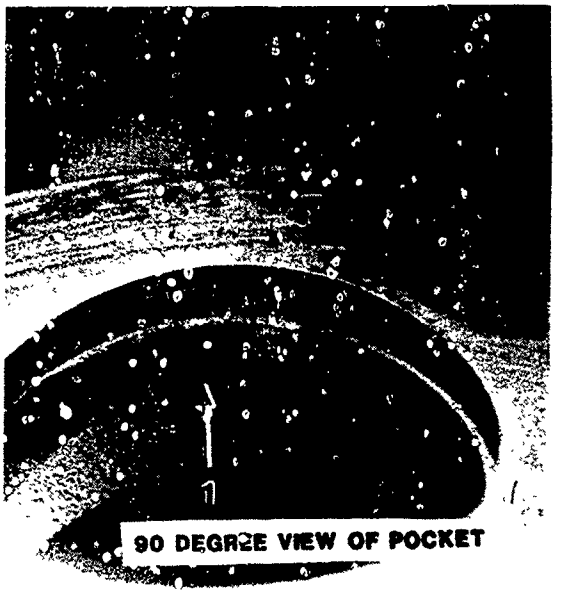

ing clearance in a 7205 angular contact can result in bearing seizure, since the initial diametral clearance is fixed. Clearly, correct interpretation of four ball test results and full scale bearing tests are required to obtain a successful solid lubricated bearing.

The major difficulties in analyzing and designing a high speed, solid lubricated bearing stems from the dichotomy of functions the cage must perform and the lack of design data at the temperatures, pressures, and speeds a solid lubricated bearing encounters. The cage must (1) supply lubricant (2) maintain spacing of the rolling elements. Unfortunately, solid lubricants generally rely on a low shear strength to provide a transfer lubricant to the rolling elements. The lubrication and strength requirements of the cage have resulted in novel cage systems, including shrouded cages, cages containing lubricant reservoirs, fiber reinforced cages, lubricant impregnated cages, and segmented cages.

In addition to the obvious difficulties associated with cage design, design of the bearing internal geometry and selection of the bearing materials will have a significant influence on bearing performance. The following subsections present design guidelines for a solid lubricated angular contact bearing.

5.5.2 Material Properties

The selection of hot pressed silicon nitride for the bearing rings and balls is advantageous when designing a high temperature solid lubricated bearing. The corrosion and oxidation resistance of a ceramic is necessary for long term high temperature applications. However, two other physical characteristics of silicon nitride which significantly improve the probability of success should be mentioned, thermal expansion and elastic modulus. A low thermal expansion coefficient minimizes the change in contact angle and diametral clearance as the thermal gradient between the inner ring and outer ring increases. In a typical bearing, the inner ring is subjected to a higher equilibrium temperature than the outer ring; therefore, bearing diametral clearance decreases. As can be seen in Figure 21, the thermal expansion coefficient has a significant effect of the predicted maximum ΔT that a bearing can survive.

The retention of a high elastic modulus of silicon nitride, Figure 22, assures adequate load carrying capability and minimizes the possibility of plastic deformation of the bearing surfaces at high temperature. Plastic deformation can increase the friction coefficient due to hystersis effects which are normally considered insignificant to bearing performance. Figure 23 shows evidence of plastic deformation of the M50 steel during the solid lubricated bearing tests.

F-4185C-1-WPM

Figure 21 Effect of Thermal Gradients on Bearing Contact Angle and Contact Stress for Hybrid and Silicon Nitride Angular Contact Bearings

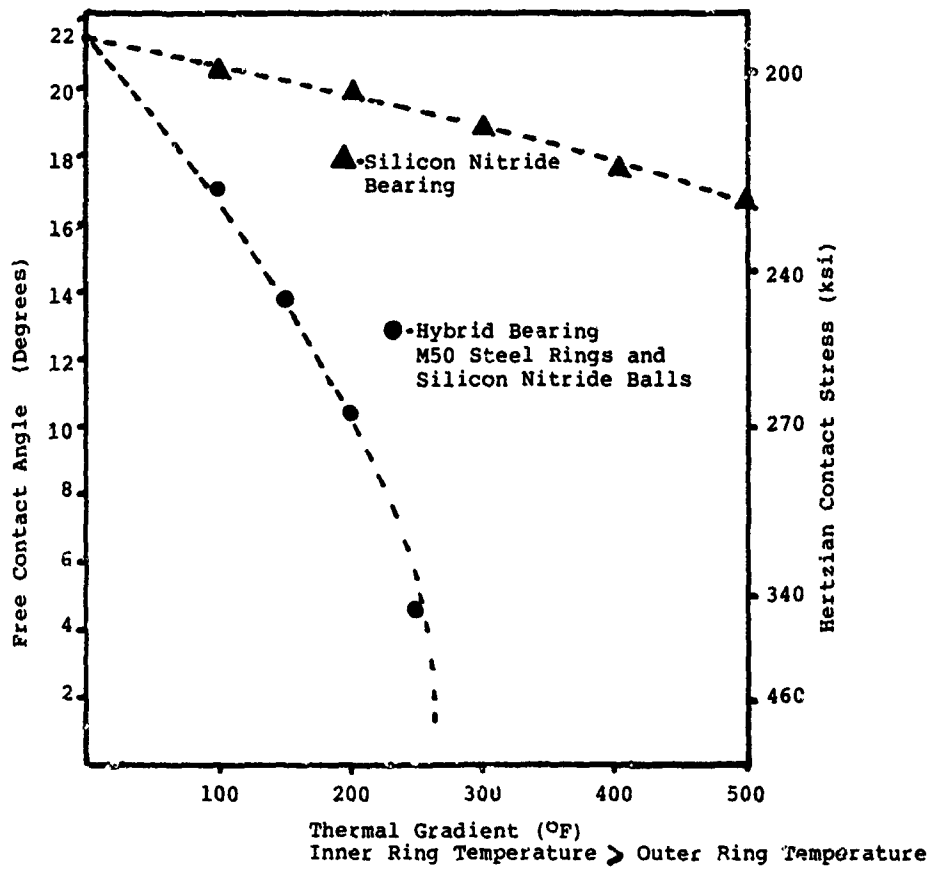

(Intentional Repeat of Figure 2, Page 8)

F-4185C-1-R100

Figure 22 Elastic Modulus of Silicon Nitride and M50 Bearing Steel as a Function of Temperature

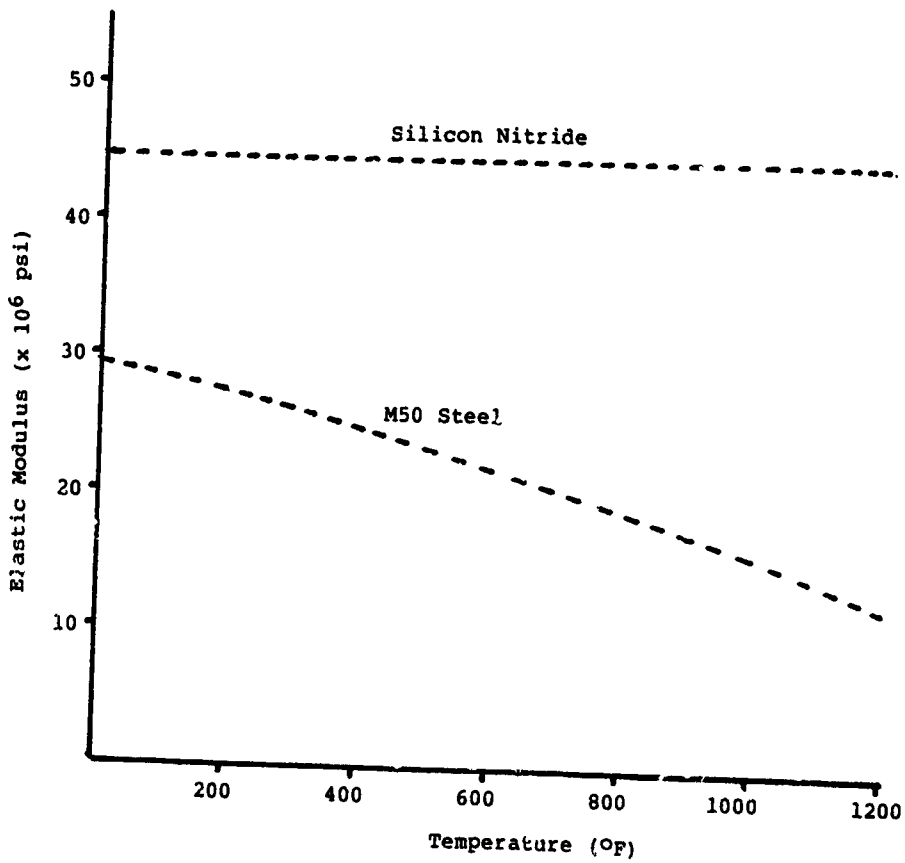

F-4185C-1-R100

Figure 23 Evidence of M50 Steel Plastic Deformation Observed by Optical Microscopy on Etched Cross Sections of an M50 Inner Ring

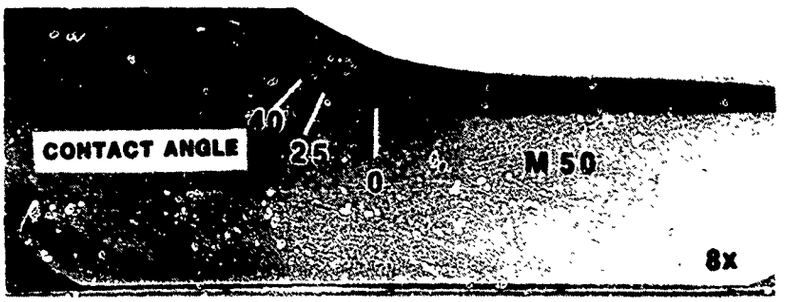

a - CARBIDES (UNDEFORMED REGION)

b - LIMITED PLASTIC DEFORMATION

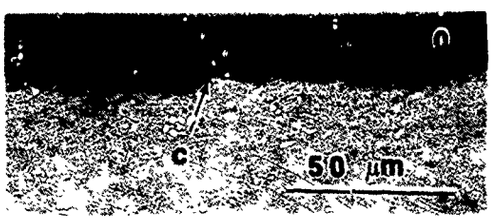

c - CRACKING AND PLASTIC DEFORMATION

F-41856-1-9100

5.5.3 Bearing Internal Geometry

The bearing internal geometry, consisting of bearing diametral clearance and the ratio of the ball groove radii to the ball diameter, has a significant influence on bearing performance. The bearing diametral clearance must be sufficient to allow incorporation of a solid lubricant coating. Estimations of the actual lubricant thickness range from 0.00001 in (0.25 μm) to 0.00013 in (5 μm) per surface. Mechanical measurements and estimations of thickness based on ball reflectivity yield values of 0.00001 in (0.25 μm) to 0.00002 in (0.6 μm), respectively. The 0.00013 in (5 μm) per surface build up was calculated using the volume of graphite removed from the cage and assuming that 100% of the lubricant was deposited on the bearing surfaces. Figure 24 shows photographic projections of the wear marks observed on the cage surfaces which were used to calculate the volume of graphite removed from the cage. This method yields an upper limit for the film thickness since graphite was observed outside the bearing envelope. Assuming that the actual solid lubricant thickness was between 0.000039 in (1 μm) and 0.00008 in (2 μm) reveals that the decrease in bearing diametral clearance will be between 0.0003 in (8 μm) and 0.0006 in (16 μm) for a Pure Carbon P2003 graphite lubricated bearing. Sufficient diametral clearance is required to obtain satisfactory solid lubricated bearing performance.

Groove radii which depart from standard bearing practice will be necessary to obtain a solid lubricated high speed bearing. Normally, groove radii are selected to maximize the bearing fatigue life at a given set of conditions. In the case of a solid lubricated bearing, the design guidelines should also include minimizing the heat generated at the inner ring and the outer ring contacts. Bissett and coauthors [13] provided an analytical prediction of the heat generated at the contacts for a 7207 bearing. Although the total heat generated due to cage - land sliding, ball-cage sliding, and the contacts may not be significantly altered, by changing the groove radii, the redistribution of the heat generated at the contacts can be improved by proper selection of the groove radii.

5.5.4 Solid Lubricated Cage Designs

5.5.4.1 Segmented Cage Design

As reported in section 3.1.2, after review of a number of conceptual cage designs, two types of segmented cage designs were selected for Phase I evaluation based on two major advantages of the segmented cage design. Hoop stresses in the graphite were eliminated by this design concept while the segmented design provided the maximum cross sectional thickness of solid lubricant possible. Although a design review did not point out any major

Figure 24 Wear Scars Produced by the Silicon Nitride Balls in the Segmented Cage Ball Pockets

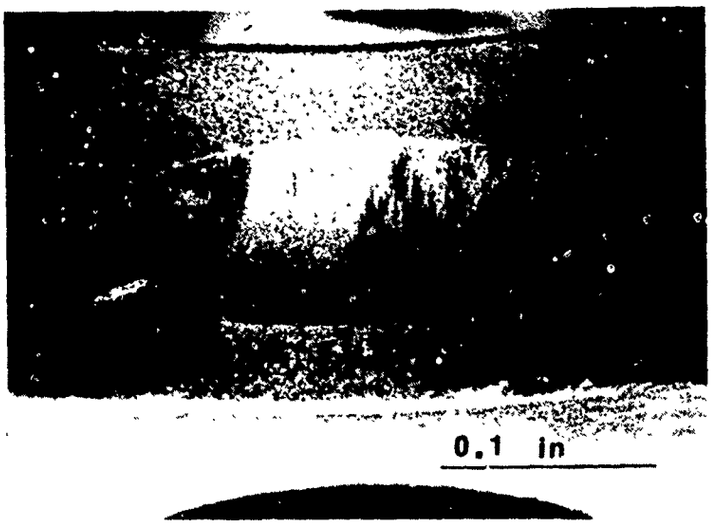

Wear mark in direction of shaft rotation.

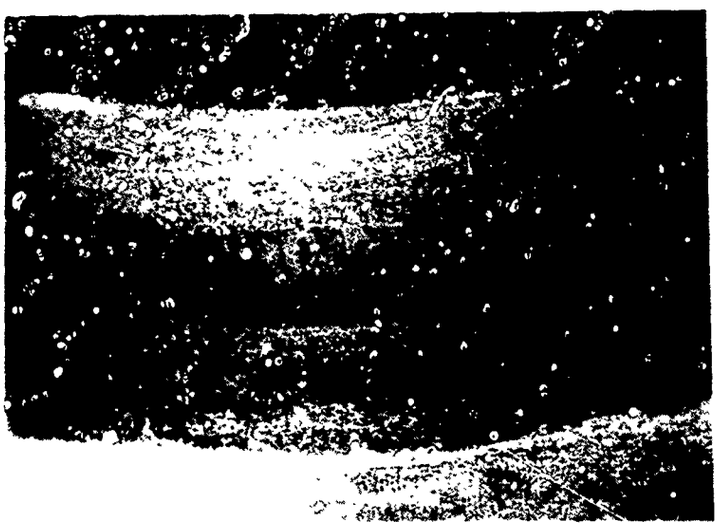

Wear mark in direction opposed to shaft rotation.

difficulties with a segmented cage, high speed testing did reveal a major problem area, that of high heat generation due to the sliding cage segments on the outer land surfaces. The radial force on the cage segment increases with the velocity squared while the heat generation increases with velocity cubed. Figure 25 shows the heat generation rate as a function of shaft speed for two coefficients of friction; $u_f = 0.05$ and $u_f = 0.15$. The turbine inlet air pressure and turbine manufacturer supplied torque characteristics were converted to the heat generation rate for the bearings. These calculations indicated that the coefficient of friction at the cage-land surface was approximately 0.05. Heat generation due to friction torque was negligible, approximately 10 watts, compared to the heat generated at the sliding interfaces.

A calculation of the PV value (pressure and velocity) based on the centrifugal loading and observed wear scar for the graphite cage segments yielded a PV number of 750,000 psi ft/min while performing satisfactorily. Typical PV numbers quoted in the literature are less than 150,000 psi ft/min for graphite, indicating that the sliding speeds and pressures are well beyond conventional design guidelines.

The evaluation of a segmented cage 30,000 rpm (3140 rad/sec) with excursions as high as 55,000 rpm (5760 rad/sec) lends credibility to the approach of developing a light weight segmented cage which closely conforms to the bearing outer ring. The higher heat generation and the high PV value were severe detriments. Therefore, it will be necessary to develop a light weight cage which closely conforms to the bearing land to decrease the PV value. Supporting the cage by an air bearing would be ideal, however, initial investigations into a cage supported by an air bearing have indicated that it is not possible to develop an air bearing capacity to completely support the cage segments.

The segmented cage concept appears feasible for 1.5 million DN and slower solid lubricated angular contact bearings. By reducing the cage mass and extending the bearing lands, it should be possible to reduce the PV value and heat generation rate to an acceptable level. The major advantage of the segmented cage system is that the design remains stable at high speed due to the piloting of the cage segments by the ball groove and the bearing lands.

5.5.4.3 Shrouded Cage Designs

The shrouded cage design investigated in Phase I failed due to a lack of axial guidance and inadequate dampening. Axial guidance can be obtained through the use of an air bearing on the faces of the graphite cage. Radial cage guidance is partially provided by the inner ring outer diameter. It should be realized that the inner diameter of the cage contacts the outer diameter of the inner ring at a single line. Therefore, the dampening available in the inner land riding cage design is limited to

Figure 25 Predicted Heat Generation Due to Cage Sliding at Two Coefficients of Friction and Calculated Heat Generation Determined from Bearing Torque

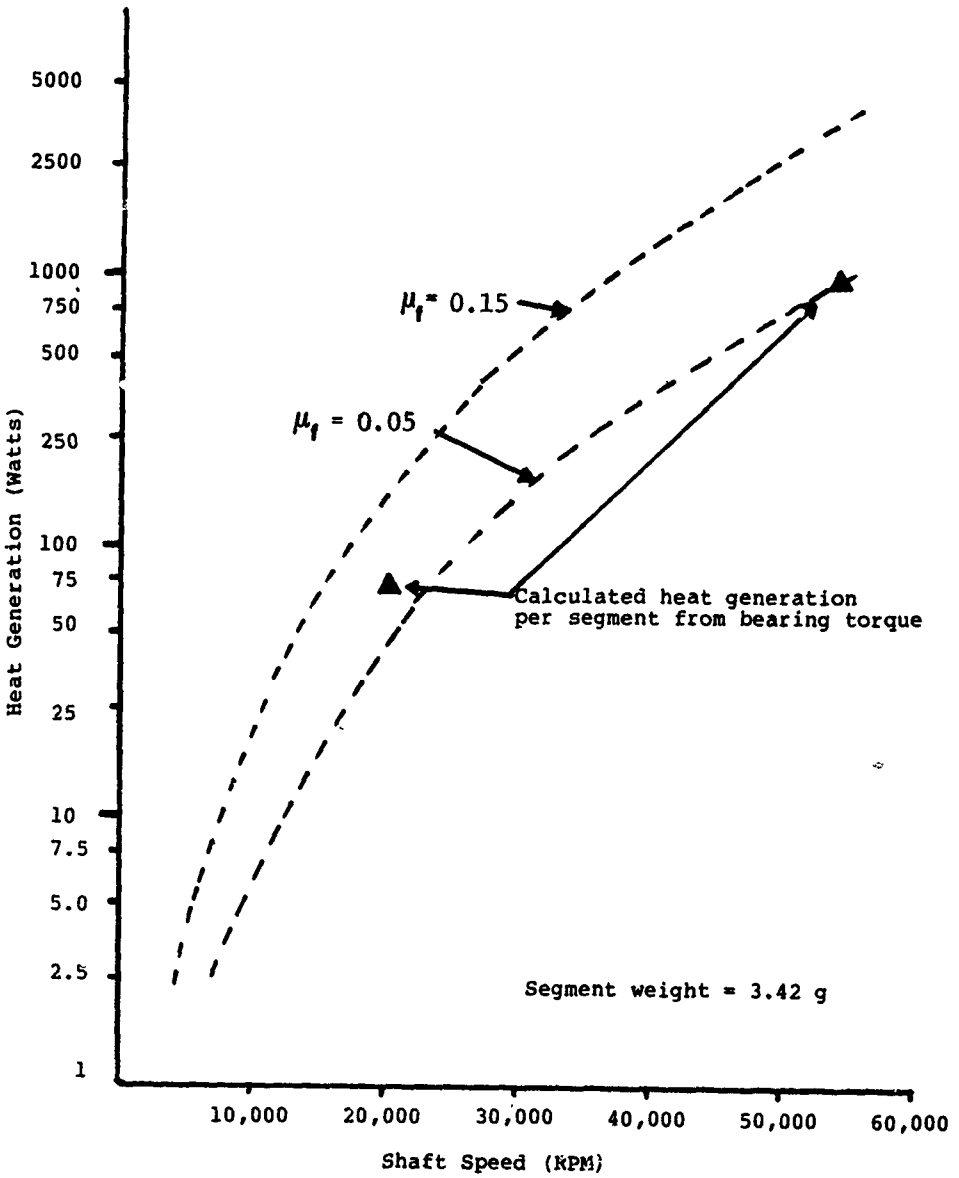

F-4185C-1-R100

this contact and ball contacts. Sliding at the inner ring also results in heat generation at a critical surface. Increased heat generation at the inner ring results in a high inner ring temperature and decreased diametral clearance. If possible, sliding should occur at the outer ring surface where the heat can be removed more easily and an increase in ring temperature results in a net gain in diametral clearance.

One possible cage design would consist of a segmented cage contained in a stainless steel shroud. The graphite segments could be clipped into position to maintain the graphite hole spacing concentric with the holes in the stainless steel shroud. Sliding would occur at the outer ring by extending the graphite beyond the stainless steel shroud as shown in Figure 26. Axial cage piloting would be obtained by utilizing an air bearing at faces of the graphite segments. Radial piloting would be achieved by the graphite sliding against the bearing outer ring. Note that the stainless steel shroud was designed to carry centrifugal loads as well as the ball pocket loading. Therefore, the graphite piloting surface would only be required to carry the unbalanced cage land force. The unbalanced cage land force is estimated to be less than 10 lbf (45 N). This cage-land force results in estimated PV values at the piloting surface less than 500,000 psi ft/min at a 55,000 rpm (5760 rad/sec) shaft speed.

Figure 26 Conceptual Design for a Segmented Outer Land Riding Cage Contained by a Metal Shroud

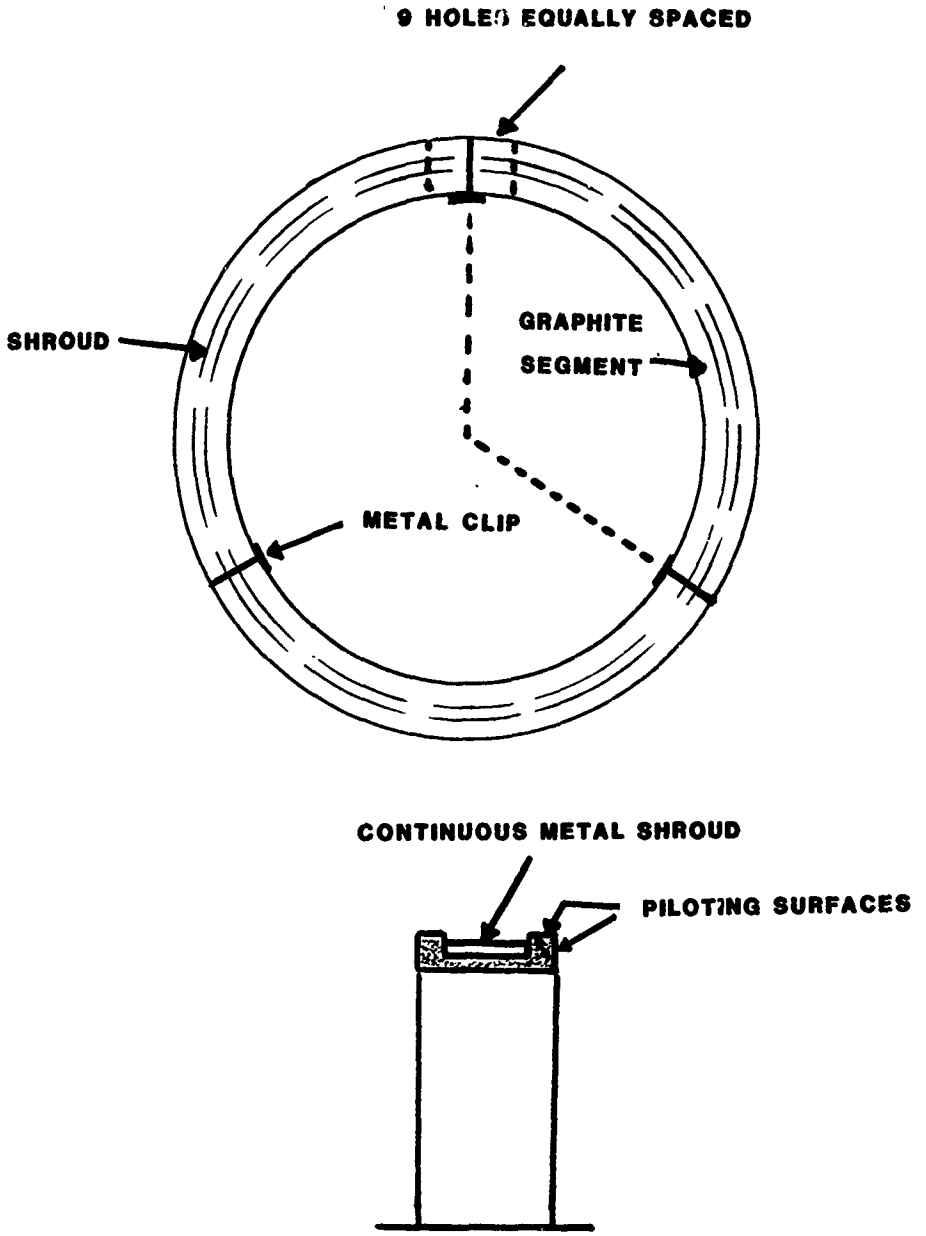

F-4185C-1-R100

6.0 Summary

The test techniques utilized in this program provided insight into the complex requirements necessary for satisfactory solid lubricated bearing performance at test conditions of interest to gas turbine engine designers. Analysis of the test results, solid lubricant cages, bearings, and the test system identified failure mechanisms and the corrective action necessary to significantly improve bearing performance. Factors contributing to the failure of the solid lubricated bearings at high speed include the following:

1. Inadequate diametral clearance to allow for a finite lubricant thickness.

2. Thermal gradients between the inner and outer rings.

3. Inability of the bearing housing design to flex and allow expansion of the outer ring.

4. High air flow rates necessary to cool the bearing can remove the solid lubricant from the bearing.

5. Inadequate dampening and piloting of shrouded cage designs.

Each of these areas can be addressed by proper modification of the cage design, bearing design, and housing design to assure satisfactory bearing performance at high speed and temperature.

Selection of the proper cage design and bearing design to minimize the heat generation at the inner ring while providing adequate cage dampening will be necessary in order to demonstrate high speed, solid lubricated bearings. Two cage design approaches appear to have potential for providing the required lubricant while maintaining adequate dampening. A segmented cage design and a shrouded segmented cage design appear to have potential for high speed applications with existing technology.

The selection of the solid lubricant, Pure Carbon P2003 graphite, appears satisfactory based on the previous four ball test results [3] and the 7205 bearing tests conducted during the present program. This graphite's light weight, relatively high strength, and excellent filming tendencies would be difficult to improve upon for high temperature solid lubricated bearing operation.

7.0 Recommendations

1. Demonstrate high speed solid lubricated bearings in angular contact using existing solid lubricants and materials. The low thermal expansion coefficient of silicon nitride will reduce the tendency for bearing seizure, while graphite transfer films provide adequate lubricant films.

2. Continue the investigation of solid lubricant cage design concepts with emphasis on outer land riding segmented cages, and shrouded segmented cages axially piloted by air bearings.

3. Future research into higher temperature (1000°F) and higher speed (55,000 rpm for a 7205 bearing) will undoubtedly require improved solid lubricants and cage designs. Material research emphasis should be directed at solid lubricant materials which melt at the high temperatures experienced in the contact, and thereby achieving very low coefficients of friction. Consideration should also be given to solid lubricant retainers fabricated from high strength, porous ceramic materials. The low thermal expansion coefficient and high elastic modulus of ceramics will be necessary to insure adequate piloting and achieve carefully controlled dimensions over the wide temperature range solid lubricated bearings are expected to perform.

8.0 References

1. F. R. Morrison, J. Pirvics, and T. Yonushonis, "Establishment of Engineering Design Data for Hybrid Steel/Ceramic Ball Bearings," Naval Air Systems Command, Contract No. N00019-78-C-0304, SKF Report No. AL79T033, (1979).

2. F. R. Morrison, and T. Yonushonis, "Establishment of Engineering Design Data for Hybrid Steel/Ceramic Ball Bearings: Phase II," Naval Air Systems Command, Contract No. N00019-79-C-0418, SKF Report No. AT80T042, (1980).

3. T. M. Yonushonis, "Dry Lubrication of High Temperature Silicon Nitride Rolling Contacts," Naval Air Systems Command, Contract No. N00019-79-C-0612, SKF Report No. AT80C040, (1980).

4. K. M. Taylor, L. B. Sibley, and J. C. Lawrence, "Development of a Ceramic Rolling Contact Bearing for High Temperature Use," Wear 6 (1963), 226-240.

5. D. J. Boes and J. S. Cunningham, "The Effects of Design Parameters and Lubricants on the Performance of Solid Lubricated, High Speed--High Temperature Bearings," Westinghouse Research Laboratories Scientific Paper No. 68-9B-5-LUBER-P1, (1968).

6. R. D. Dayton, M. A. Sheets, and J. B. Schrand, "Evaluation of Solid Lubricated Ball Bearing Performance," ASLE Transactions, 21, 3, 211-216.

7. L. J. Nypan, "Separator to Ball Contact Force Measurements in Solid Lubricated Bearings," Final Report, Hughes P.O. 04-406060-FS5, California State University, 1980 in "Solid Lubricated Rolling Element Bearing Status Report No. 4 & 5" DARPA order 3576, AFWAL/MLBT Contract F33615-78-C-5196.

8. R. Heemksherk, "Cage Stability in Angular Contact Ball Bearings for Ultra High Speed Grinding Spindles: A Design Concept," SKF Engineering & Research Centre B.V., Report No. NL80T506, (1980).

9. E. P. Kingsbury, "Torque Variations in Instrument Ball Bearings," ASLE Transactions, 9 (1965) 435-441.

10. J. W. Kannel and S. S. Bupara, "A Simplified Model of Cage Motion in Angular Contact Bearings Operating in the EHD Lubrication Regime," Journal of Lubrication Technology 100 (1978) 395-403.

11. D. J. Boes, "Development of Lightweight Solid Lubricated Bearing Retainers," Air Force Aero Propulsion Laboratory Contract F33615-77-C-2027, Westinghouse Research and Development Center, Report No. AFAPL-TR-78-72 (1978).

12. G. J. Adams and J. R. Jones, "The Effect of Retainer Geometry on the Stability of Ball Bearings," presented at the 30th ASLE Annual Meeting, May 5-8, 1975.

13. P. R. Bissett, R. L. Downey, and R. A. Solomon, "High Temperature, High Speed Solid Lubricated Bearing Technology Phase I - Heat Transfer," Air Force Aero Propulsion Laboratory Technical Report AFAPL-TR-7Y-77, AiResearch Manufacturing Report 74-410569-1 (1974).

APPENDIX A

7205 Bearing Tests

Test A:

Test Objectives	Check manual control system, air turbine, and bearing load system.
Test Approach	Two standard 52100 steel 7205 C/P4 DGA bearings were tested with oil mist lubrication by slowly accelerating the air turbine to 55,000 rpm (5760 rad/sec). The oil mist pressure was set at 22 psi for the turbine and 10 psi to the test bearings. An axial load of 100 lbf (450 N) was applied to the test bearings. Turbine speed was manually controlled by a series of air valves.
Test Summary	An erratic turbine speed was observed during the first six minutes of test. Increasing the oil mist pressure from 10 psi to 17 psi decreased the speed variation to $\pm$ 1000 rpm at 27,000 rpm. However, accelerating the air turbine to 35,000 rpm increased the speed variation to $\pm$ 3000 rpm. A total of 226 minutes was recorded on the test bearings. Ten minutes of test at 50,000 rpm were conducted prior to system shut down due to an increasing bearing temperature.
Inspection Summary	The test bearing contained in the load plug experienced lubrication distress. The ball wear track was observed at an incorrect contact angle, possibly indicating an incorrect load application on the bearings.

Test B:

Test Objectives	Same as Test A and verification of proper load application on test bearings.
Test Approach	Same as Test A. Oil mist pressure was increased to 40 psi to the test bearings.

Test Summary

A cyclic test speed was observed at constant turbine inlet pressures indicating torque changes in the oil lubricated test bearings. The steel bearings were tested at 55,000 rpm (5760 rad/sec) for four minutes prior to bearing seizure. The maximum outer ring temperature recorded was 290°F (140°C).

Inspection Summary

Inspection of the bearing rings revealed that both bearings were properly loaded. Failure of the load plug bearing was due to inadequate lubrication.

Test 1

Test Objective

Evaluate two 7205 hybrid bearings containing segmented graphite cage design L-23845.

Test Conditions

- 100 lbf (450 N) axial load applied equally to both bearings
- housing temperature 200°F (93°C)
- 4 SCFM cooling air to bearing cavity
- 0.0007 in. (18 μm) diametral clearance after shaft interference fit

Test Summary

After increasing the turbine speed to 10,000 rpm (1050 rad/sec), the bearing outer ring temperatures had equilibrated at 250°F (120°C). Increasing the speed to 20,000 rpm (2100 rad/sec) resulted in an outer ring temperature of 390°F (200°C). An additional increase in test speed to 30,000 rpm (3150 rad/sec) resulted in bearing seizure. A maximum inner ring temperature of 600°F (315°C) was recorded. The total test time was 13 minutes.

Inspection Summary	The M50 rings and silicon nitride balls were damaged due to bearing seizure. The segmented cage was in good condition. The heavy wear observed on the cage outer diameter was related to the poor land surface finish, approximately 60 μ in. RMS.

Test 2-1

Test Objective	Determine if preferentially heating outer rings will increase bearing clearance and if reduced load will improve bearing performance for hybrid bearing containing segmented cage design L-23845.
Test Conditions	Same as Test 1 with exception that load was reduced to 25 lbf (110 N).
Test Summary	Variations in cooling air flow and housing temperature did not result in a temperature differential between the inner and outer rings. Bearing speed was increased gradually to 32,000 rpm (3350 rad/sec) prior to bearing seizure.
Inspection Summary	All components were in excellent condition.

Test 2-2

Test Objective	Evaluate cage design L-23845.
Test Conditions	• 25 lbf (110 N) axial load applied to test bearings • bearing housing temperature was 80°F (27°C) • air cooling supplied to bearing cavity at 4 SCFM.
Test Summary	The turbine speed was gradually increased to 40,000 rpm (4190 rad/sec) over a 60 second period prior to evidence of impending bearing seizure. A maximum temperature of 450°F (230°C) was recorded at the inner ring and 300°F (150°C) at the outer ring.

Inspection Summary — Test rig was not disassembled. The segmented cage was visually inspected through the infrared pyrometer port. This cage appeared undamaged.

Test 2-2

Test Objective — Repeat of Test 2-1.

Test Conditions

- Same as Test 2-2 with exception that air cooling flow rate was increased to 12 SCFM.

Test Summary — The turbine speed was held between 10,000 RPM and 12,000 RPM for 75 minutes. Test was stopped due to bearing temperatures increasing.

Inspection Summary — Same as Test 2-2.

Tests 2-4, 2-5, and 2-6 — Repeat of 2-1.

Test Summary

2-4
- Accelerated turbine from 0 to 52,000 RPM in 5 seconds then air supply cut to turbine. I.R. 480°F - O.R. 180°F Δ T = 300°F. Front bearing cage segments OK.

2-5
- Accelerated from 0.70 to 52,000 RPM in 8 seconds then air supply cut to turbine
- I.R. = 600°F O.R. = 230°F Δ T = 370°F

2-6
- Accelerated from 0 to 54,000 RPM in 12 seconds air supply increased accidentally resulting in greatly increased air pressure to turbine as bearing seized.
- I.R. = 700°F O.R. = 380°F ΔT = 320°F

Inspection Summary — Two segments survived Test 2-6. Three silicon nitride balls exhibited cracks due to high loading.

F-4185C-4-R100

Tests 3-1, 3-2, and 3-3

Test Objective

Evaluate cage design L-23875 with bearing having increased diametral clearance.

Test Conditions

- 25 lbf (110 N) axial load
- Housing temperature 80°F (92 °C) for test 3-1.
- Air cooling supplied at 4 SCFM.

Test Summary

3-1
- Test speed was held to 10,000 rpm (1050 rad/sec) while allowing bearing temperatures to stabilize. After approximately 10 minutes the outer ring temperatures had stabilized at 158°F (70°C). Increasing the speed to 20,000 rpm (2100 rad/sec) resulted in an outer ring temperature of 250°F (120°C) and an inner ring temperature of 400°F (205°C). The system was shut off to check the test bearings. No seizure of the test bearings was noted.

3-2
- The housing heaters were turned on and the housing temperature was allowed to stabilize at 250°F (120°C) prior to starting the air turbine. Test speed was rapidly increased to 23,000 rpm (2410 rad/sec) A maximum inner ring temperature of 550°F (290°C) and an outer ring temperature of 400°F (205°C) was recorded.

3-3
- In Test 3-3, the bearings were accelerated to 33,000 rpm (3400 rad/sec) when high temperatures were observed on the inner and outer rings. Monitoring the Ircon infrared pyrometer yielded at maximum inner ring temperature of 750°F (400°C). The thermocouples recorded a maximum outer ring temperature of 550°F (290°C) prior to test shut down.

Inspection Summary

Visual inspection of the load plug bearing cage through the pyrometer port revealed that the segmented cages had survived test 3-1 and 3-2. Inspection after test 3-3 revealed that one cage segment had fractured. Disassembly revealed that one cage segment in the load plug bearing had fractured axially and circumferentially. One other segment also exhibited signs of distress. This segment was circumferentially cracked through the cage webs, but remained intact. The cage segments from the bearing in the drive portion of the rig were undamaged. The silicon nitride balls and M50 rings were in excellent condition after this test series.

Tests 4-1, 4-2, 4-3, and 4-4

Test Objectives

Evaluate cage design L-23875 with an increased airflow to the test bearings.

Test Conditions

- 25 lbf (110 N) axial load
- Housing temperature 80°F (27°C)
- Air cooling supplied at 12 SCFM.
- Load plug modified by drilling two 0.25 in diameter holes through the plug to increase cooling air flow to the test bearing in the load plug. Previously all air flow exited through the 0.5 inch infrared pyrometer port.

Test Summary

4-1

- Bearing temperature equilibrated at 160°F (70°C) at 16,000 rpm (1680 rad/ sec). The turbine speed was then increased to 25,000 rpm (2620 rad/sec) when bearing seizure was imminent. The turbine was stopped to prevent bearing seizure.

F-4185C.1-R100

4-2 • Speed increased to 25,000 rpm (2620 rad/sec) then turbine by rapidly accelerating the air turbine. Recorded 450°F (230°C) inner ring temperature and 210°F (100°C) outer ring temperature prior to shutting down the air turbine. Test bearings rotated freely by hand indicating that the bearings were not damaged.

4-3 • Heated housing to 200°F (93°C) to provide clearance for outer ring to expand. After housing temperatures had stabilized, the test 4-3 was initiated by rapidly accelerating the turbine to 26,000 rpm (2720 rad/sec). Noise generated at 26,000 rpm indicated that the bearing was beginning to seize; therefore, the test was stopped.

4-4 • Increased air turbine speed to 55,000 rpm (5160 rad/sec) in 15 seconds in a repeat of test series 2-4, 2-5, and 2-6. Bearings seized immediately resulting in immediate speed reduction.

Inspection Summary — All segmented cages had fractured due to bearing seizure in Test 4-4. Inspection of the silicon nitride balls revealed that three balls were cracked during test 4-4.

Test 5

Test Objective — Evaluate segmented cage design L-23845 and shrouded cage L-23846 at low speed.

Test Conditions

- 100 lbs (450 N) axial load
- Housing temperature 80°F (27°C)
- Air cooling supplied at 11 SCFM.

Test Summary — The test bearings were tested at 5000 rpm (525 rad/sec) for 20 minutes, then speed decreased to 2,000 rpm at a constant turbine air inlet pressure. The turbine eventually stopped at a constant air pressure indicating an increase in bearing torque.

Inspection Summary	The shrouded graphite cage exhibited very little evidence of wear in the ball pockets. The steel rings for this bearing did not appear to have a graphite coating. The segmented cage exhibited considerably more wear due to the balls sliding against the cage pocket.

Test 6

Test Objectives	Repeat of Test 5.
Test Conditions	Same as test 5.
Test Summary	Started test rig accelerated turbine to 10,000 rpm. Turbine stopped after 2.5 minutes of testing at a turbine inlet pressure of 6.5 psi. Restarted the turbine by rotating the shaft by hand. Turbine speed varied from 7,000 rpm to 1,000 rpm over the next 20 minutes. Variations in speed from 5,000 to 13,000 rpm were observed at an increased turbine inlet pressure of 10 psi over the next 78 minutes. The test system was stopped after 100 minutes of test at low speed.
Inspection Summary	Both bearings were in excellent condition after test 6. Graphite cage pocket wear for the shrouded cage was considerably heavier than in test 5. Very little graphite was observed on the steel ring surfaces possibly indicating that the graphite was removed by the cooling air flow through the bearings.

Test 7

Test Objectives

Continued evaluation of segmented cage design L-23845 and shrouded cage design L-23846.

Test Conditions

- 100 lbf (450 N) axial load
- no cooling air supplied to bearing cavity

Test Summary

Tested the bearings for 33 minutes at shaft speeds between 5,000 rpm and 22,000 rpm. Test was halted after 33 minutes due to the silicon nitride balls contacting the stainless steel shroud. The following table presents the bearing temperatures recorded for the bearing containing the segmented cage.

Time (min)	Speed (RPM)	Inner Ring Temp °F	Outer Ring Temp °F	ΔT
0	5,000	350	150	
6	10,000	350	250	100
13	10,000	420	290	130
16	13,000	450	310	140
20	14,000	505	340	165
24	14,000	550	375	175
28	17,000	580	425	155
29	18,000	595	430	160
30	18,000	630	455	175
33	15,000	680	490	190

85C-1-R100

Inspection Summary

Graphite coating prevalent on all bearing surfaces with the segmented cage. The cage design L-23845 was in excellent condition, while in the shrouded design the balls had contacted the steel shroud. All other bearing components were in excellent condition.

F-4185C-1-R100

Test 8

Test Objectives	Evaluate two shrouded cages simultaneously.
Test Conditions	• 100 lbf (450 N) axial load • No cooling air
Test Summary	Bearing test could not be conducted due to cage unbalance at low speed. Severe "rattling" of the shrouded cages prevented the test.
Inspection Summary	Graphite cage pockets had a small wear mark. Graphite transfer films were not visible on the M50 bearing surfaces.

F-4185C-1-R100

DISTRIBUTION LIST FOR N00019-80-C-0565

	NO OF COPIES
Commander Naval Air Systems Command Washington, DC 20361 Attention: AIR-00D4 8 AIR-310C 1 AIR-330 1 AIR-536 1 AIR-320A 1 AIR-5304C1 5	17
Office of Naval Research 800 N. Quincy ST Arlington, VA 22217 Attention: Code 471	1
Commander Naval Surface Weapons Center White Oak Silver Spring, MD 20910 Attention: Code R31	1
Director Naval Research Laboratory Washington, DC 20375 Attention: Code 6360	1
Commanding Officer David W Taylor Naval Ship Research & Development Center Annapolis, MD 21412 Attention: W. SMITH, Code 2832	1
Commanding Officer Naval Air Propulsion Center Trenton, NJ 08628 Attention: R. Valeri, Code PE 72	1
Commander Naval Ocean Systems Center San Diego, CA 92152 Attention: Dr. J. Stachiw, Code-5204(B)	1
Commander Naval Air Development Center Warminster, PA 18974 Attention: Code 6061	1
Officer in Charge of Construction Civil Engineering Laboratory Naval Facility Engineering Command Detachment Naval Construction Battalion Center Port Hueneme, CA 93043 Attention: Stan Black, Code L40	1

Commander 4
Air Force Wright Aeronautical Labortories
Wright-Patterson Air Force Base
Dayton, OH 45433
Attention: Dr. J. Dill POSL 1
Dr. H. Graham MLLM 1
Mr. B. D. McConnell MLBT 1
MS. K. Lark KLTM 1

Brookhaven National Laboratory 1
Upton, NY 11973
Attention: Dr. D. Van Rooyen

Director 1
Applied Technology Laboratory
US Army Research & Technology Laboratories
Fort Eustis, VA 23604
Attention: DAVDL-ATL-ATP (Mr. Pauze)

US Army Research Office 1
Box CM, Duke Station
Durham, NC 27706
Attention: CRCARD

US Army MERDC 1
Fort Belvoir, VA 22060
Attention: SMEFB-EP (W. McGovern)

Army Materials and Mechanics Research Center 1
Watertown, MA 02172
Attention: Dr. R. N. Katz

NASA Headquarters 1
Washington, DC 20546
Attention: C. F. Bersch, RTM-6

NASA Lewis Research Center 3
21000 Brookpark RD
Cleveland, OH 44135
Attention: Dr. E. Zaretsky (6-1) 1
W. A. Sanders (49-1) 1
and Dr. T. Hergell

Defense Advanced Research Project Office 1
1400 Wilson Blvd
Arlington, VA 22209
Attention: Dr. Van Reuth

Inorganic Materials Divsision 1
Institute for Materials Research
National Bureau of Standard
Washington, DC 20234

Department of Engineering 1
University of California
Los Angeles, CA 90024
Attention: Profs. J.W. Knapp and G. Sines

Engineering Experiment Station
Georgia Institute of Technology
Atlanta, GA 30322
Attention: J.D. Walton

1

University of Illinois
College of Engineering
204 Ceramics Building
Urbana, IL 61801
Attention: Sherman D. Brown
Department of Ceramic Engineering

1

Department of Engineering Research
North Carolina State University
Raleigh, NC 27607
Attention: Dr. H. Palmour

1

Ceramic Science and Engineering Section
Pennsylvania State University
University Park, PA 16802
Attention: Dr. R. E. Tressler

1

Rensselaer Polytechnic Institute
110 Eighth Street
Troy, NY 12181
Attention: R.J. Diefendorf

1

School of Ceramics
Rutgers, The State University
New Brunswick, NJ 08903

1

Virginia Polytechnic Institute
Minerals Engineering
Blacksburg, VA 20460
Attention: Dr. D. P. H. Hasselman

1

Advanced Mechanical Technology Inc
141 California Street
Newton, MA 02158
Attention: Dr. Walter D. Syniuta

1

Aerospace Corporation
Materials Laboratory
P.O. Box 95085
Los Angeles, CA 90045

1

Supervisor, Materials Engineering
Department 93-39M
AiResearch Manufacturing Company of Arizona
402 South 36th Street
Phoenix, AZ 85034

1

Materials Development Center
AVCO Systems Division
Wilmington, MA 01887
Attention: Tom Vasilos

1

Lycoming Division
AVCO Corporation
Stratford, CT 06497
Attention: Mr. D. Wilson — 1

Barden Corporation
Danbury, CT 06810
Attention: Mr. K. MacKenzie — 1

Batelle Memorial Institute
505 King Avenue
Columbus, OH 43201
Attention: Ceramics Department — 1
Metal & Ceramic Information Center — 1 — 2

Bell Helicopter Textron
P.O. Box 482
Fort Worth, TX 76101
Attention: R. Battles — 1

The Boeing Company
Materials and Processes Laboratory
Aerospace Group
P.O. Box 3999
Seattle, WA 98124
Attentioon: J. VanWyk — 1

Reseach and Development Division
Carborundum Company
Niagra Falls, NY 14302
Attention: Mr. C. McMurty — 1

Caterpillar Tractor Company
Technical Center
East Peoria, IL 61611
Attention: A. R. Canady — 1

Ceramic Finishing Company
Box 498
State College, PA 16801 — 1

Ceradyne Inc
Box 1103
Santa Ana, CA 92705 — 1

Chrysler Corporation
Research Department
Box 1118-Bldg 128-3
CIMS 418-37-18 - Dept 9520
Detroit, MI 48288
Attention: Mr. Norm Sparks — 1

Coors Porcelain Company
600 Ninth Street
Golden, CO 80401
Attention: Research Department — 1

Cummings Engine Company
Columbus, IN 47201 1900 McKinley Ave.
Attention: Mr. R. Kamo, Director of Research — 1

Curtiss-Wright Company 1
Wright Aeronautical Division
One Passaic Street
Woodridge, NJ 07075

Fafnir Bearing Company 1
Division Textron Corporation
27 Booth Street
New Britian, CT 06050

F.A.G. Bearing Corporation 1
70 Hamilton Avenue
Stamford, CT 06904
Attention: Thomas Trombetto

Federal-Mogul Corporation 1
Anti-Friction Bearing R&D Center
3980 Research Park Drive
Ann Arbor, MI 48104
Attention: D. Glover

Fiber Materials, Inc 1
Biddeford Industrial Park
Biddeford, ME 04005
Attention: Dr. H. Dean Batha

FMC Corporation 1
Bearing Division
7601 Rockville Drive, Box 85
Indianapolis, IN 46224
Attention: E. E. Pfoffenberger
Manager, Engineering Analysis

Product Development Group 1
Ford Motor Company
20000 Rotunda Drive
Dearborn, MI 28121
Attention: Mr. E. Fisher

Aircraft Engine Group 1
Technical Information Center
Main Drop N-32, Building 700
General Electric Company
Cincinnati, OH 45215

Metallurgy and Ceramics Research Department 1
General Electric R&D Laboratories
P.O. Box 8
Schenectady, NY 12301

Space Sciences Laboratory 1
General Electric Company
P.O. Box 8555
Philadelphia, PA 19101

Detroit Diesel Allison Division 1
General Motors Corporation
P.O. Box 894
Indianapolis, IN 46206
Attention: Dr. M. Herman

NDH Division
General Motors Corporation
Hayes Street
Sandusky, OH 44870
Attention: H. Woerhle — 1

Hughes Aircraft Company
Culver City, CA 90230
Attention: M. N. Gardos
11940 W. Jefferson Blvd.
MS D133 - Bldg. 6 — 1

IIT Research Institute
10 West 35th Street
Chicago, IL 60616
Attention: Ceramics Division — 1

Industrial Tectonics, Inc
18301 Santa Fe Avenue
Compton, CA 90224
Attention: Hans R. Signer — 1

Kaweki-Berylco Industry
Box 1462
Reading, PA 19603
Attention: Mr. R. J. Longnecker — 1

Research and Development Division
Arthur D. Little Company
Acorn Park
Cambridge, MA 02140 — 1

Litton Guidance & Control Systems
5500 Canoga Avenue
Woodland Hills, CA 91364
Attention: Robert A. Westerholm, Mail Station 87 — 1

Mechanical Technology, Inc
968 Albany-Shaker Road
Latham, NY 12110
Attention: Dr. E. F. Finkin — 1

Norton Company
Industrial Ceramics Division
One New Bond Street
Worcester, MA 01606
Attention: Dr. M. Torti — 1

North American Rockwell Science Center
P. O. Box 1085
Thousand Oaks, CA 91360 — 1

Rollway Bearing Company
Division Lipe Corporation
7600 Morgan Road
Liverpool, NY 13099
Attention: B. Dalton — 1

Ceramic Division
Sandia Corporation
Albuquerque, NM 87101 — 1

Solar Turbines International
P. O. Box 80966
San Diego, CA 92138
Attention: G. W. Hosang

1

Southwest Research Institute
P. O. Drawer 28510
San Antonio, TX 78228

1

Materials Sciences & Engineering Laboratory
Stanford Research Institute
Menlo Park, CA 94025
Attention: Dr. Cubiciotti

1

Teledyne CAE
1330 Laskey Road
Toledo, OH 43601
Attention: Hugh Gaylord

1

The Timken Company
Canton, OH 44706
Attention: R. Cornish 1835 Dueber Ave. S.W.

1

Marlin Rockwell, Division of TRW
Jamestown, NY 14701
Attention: John C. Lawrence & A. S. Irwin

1

Union Carbide Corporation
Parma Technical Center
P. O. Box 6116
Cleveland, OH 44101

1

Materials Sciences Laboratory
United Technologies
East Hartford, CT 06101
Attention: Dr. J. J. Brennan

1

Pratt & Whitney Aircraft Group
Government Products Division
United Technologies
P. O. Box 2691
West Palm Beach, FL 33402
Attention: Mr. J. Miner

1

United Technologies Research Center
East Hartford, CT 06108
Attention: F. L. Ver Snyder

1

Astronuclear Laboratory
Westinghouse Electric Corporation
Box 10864
Pittsburgh, PA 15236

1

Westinghouse Research Laboratories
1310 Beulah Road
Churchill Borough
Pittsburgh, PA 15235
Attention: Dr. R. Bratton

1

Williams International Corporation 2280 W. Maple Rd.
Walled Lake, MI 48088

1